Electrochemical Reduction of CO_2 to Value-Added Chemicals on Zn/Cu Alloy
Catalysts Prepared by Electrodeposition

Mr. Phongsathon Klongklaew

จุฬาลงกรณ์มหาวิทยาลัย
CHULALONGKORN UNIVERSITY

A Thesis Submitted in Partial Fulfillment of the Requirements
for the Degree of Master of Engineering in Chemical Engineering
Department of Chemical Engineering
FACULTY OF ENGINEERING
Chulalongkorn University
Academic Year 2019

การรีดักชันทางเคมีไฟฟ้าของแก๊สคาร์บอนไดออกไซด์เป็นสารเคมีมูลค่าเพิ่มบนตัวเร่งปฏิกิริยาโลหะ
ผสมสังกะสี/ทองแดงที่เตรียมโดยการพอกพูนด้วยไฟฟ้า

นายพงศธร คล่องแคล่ว

จุฬาลงกรณ์มหาวิทยาลัย
CHULALONGKORN UNIVERSITY

วิทยานิพนธ์นี้เป็นส่วนหนึ่งของการศึกษาตามหลักสูตรปริญญาวิศวกรรมศาสตรมหาบัณฑิต
สาขาวิชาวิศวกรรมเคมี ภาควิชาวิศวกรรมเคมี
คณะวิศวกรรมศาสตร์ จุฬาลงกรณ์มหาวิทยาลัย
ปีการศึกษา 2562
ลิขสิทธิ์ของจุฬาลงกรณ์มหาวิทยาลัย

Thesis Title	Electrochemical Reduction of CO_2 to Value-Added Chemicals on Zn/Cu Alloy Catalysts Prepared by Electrodeposition
By	Mr. Phongsathon Klongklaew
Field of Study	Chemical Engineering
Thesis Advisor	Professor JOONGJAI PANPRANOT, Ph.D.
Thesis Co Advisor	Associate Professor YUTTANANT BOONYONGMANEERAT, Ph.D.

Accepted by the FACULTY OF ENGINEERING, Chulalongkorn University in Partial Fulfillment of the Requirement for the Master of Engineering

.... Dean of the FACULTY OF
ENGINEERING
(Professor SUPOT TEACHAVORASINSKUN, D.Eng.)

THESIS COMMITTEE

.... Chairman
(Assistant Professor AMORNCHAI ARPORNWICHANOP, D.Eng.)

.... Thesis Advisor
(Professor JOONGJAI PANPRANOT, Ph.D.)

.... Thesis Co-Advisor
(Associate Professor YUTTANANT BOONYONGMANEERAT, Ph.D.)

.... Examiner
(Chutimon Satirapipathkul, Ph.D.)

.... External Examiner
(Assistant Professor Okorn Mekasuwandumrong, Ph.D.)

พงศธร คล่องแคล่ว : การรีดักชันทางเคมีไฟฟ้าของแก๊สคาร์บอนไดออกไซด์เป็นสารเคมี
มูลค่าเพิ่มบนตัวเร่งปฏิกิริยาโลหะผสมสังกะสี/ทองแดงที่เตรียมโดยการพอกพูนด้วย
ไฟฟ้า. (Electrochemical Reduction of CO_2 to Value-Added Chemicals on
Zn/Cu Alloy Catalysts Prepared by Electrodeposition) อ.ที่ปรึกษาหลัก : ศ. ดร.
จูงใจ ปั้นประณต, อ.ที่ปรึกษาร่วม : รศ. ดร.ยุทธนันท์ บุญยงมณีรัตน์

ในงานนี้ศึกษาตัวเร่งปฏิกิริยาทางไฟฟ้าโลหะผสมสังกะสี/ทองแดงที่เตรียมโดยการพอก
พูนทางไฟฟ้าของสังกะสีบนแผ่นทองแดงและการพอกพูนทางไฟฟ้าของสังกะสีและทองแดงบน
แผ่นทองแดงในอ่างพอกพูนทางไฟฟ้าที่แตกต่างกันประกอบด้วยอ่างโซเดียมคลอไรด์และอ่างไฮโดร
คลอริกด้วยเวลาพอกพูน 60 และ 200 วินาที ในปฏิกิริยารีดักชันแบบใช้ไฟฟ้าช่วยของ
คาร์บอนไดออกไซด์ ผลจากเทคนิคกล้องจุลทรรศน์อิเล็กตรอนแบบส่องกราดร่วมกับเอ็กซเรย์สเปก
โตรสโกปีแบบกระจายพลังงาน และการกระเจิงของรังสีเอ็กซ์แสดงว่าการพอกพูนทางไฟฟ้าส่งผล
ต่อโครงสร้างของซิงค์ (เด็นไดรท์หรือบัลคี้) ภายใต้ภาวะการดำเนินการที่ศึกษาปฏิกิริยารีดักชัน
แบบใช้ไฟฟ้าช่วยของคาร์บอนไดออกไซด์บนตัวเร่งปฏิกิริยาเหล่านี้ได้ผลิตภัณฑ์ที่เป็นก๊าซ
ประกอบด้วยคาร์บอนมอนอกไซด์และไฮโดรเจนและงผลิตภัณฑ์ของเหลวประกอบด้วยฟอร์เมท
และเอ็น-โพรพานอลจากการวิเคราะห์ด้วยเทคนิคแก๊สโครมาโตกราฟและนิวเคลียร์แมกเนติกเร
โซแนนซ์ตามลำดับ ในหมู่ตัวเร่งปฏิกิริยาที่ศึกษาสังกะสี/ทองแดง-โซเดียม200เป็นตัวเร่งปฏิกิริยา
ทางไฟฟ้าที่ดีที่สุดซึ่งผลิตคาร์บอนมอนอกไซด์สูงขณะที่ผลิตไฮโดรเจนต่ำที่ศักย์ -1.6 โวลต์ต่อซิล
เวอร์/ซิลเวอร์คลอไรด์ เพราะอนุภาคสังกะสีปกคลุมเพียงพอบนตัวถูกเปลี่ยนทองแดงและความ
ว่องไวในการเกิดปฏิกิริยามีความเสถียรสำหรับเวลาในการทดสอบปฏิกิริยา 4 ชั่วโมงถึงแม้ว่า
อนุภาคของซิงค์เด็นไดรท์จะมีขนาดใหญ่ขึ้นหลังการทำปฏิกิริยาแสดงถึงการกลับมาเกาะใหม่ของ
ซิงค์ระหว่างปฏิกิริยา ในทางตรงข้าม ตัวเร่งปฏิกิริยาซิงค์บัลคี้แสดงผลิตภัณฑ์ฟอร์เมทที่โดด
เด่น ทั้งนี้คาดว่าเป็นผลจากการที่ซิงค์บัลคี้มีสัณฐานในรูปแบบของเฮกซะโกนัลโคลสแพคที่
ส่งเสริมการเกิดฟอร์เมทผ่านการรีดักชันของสารอันตรกิริยา HCOO*

สาขาวิชา	วิศวกรรมเคมี	ลายมือชื่อนิสิต ....
ปีการศึกษา	2562	ลายมือชื่อ อ.ที่ปรึกษาหลัก ....
		ลายมือชื่อ อ.ที่ปรึกษาร่วม ....

6170217121 : MAJOR CHEMICAL ENGINEERING

KEYWORD: Electrochemical carbon dioxide reduction, Carbon monoxide production, Electrodeposition, Zinc-copper catalyst

Phongsathon Klongklaew : Electrochemical Reduction of CO_2 to Value-Added Chemicals on Zn/Cu Alloy Catalysts Prepared by Electrodeposition. Advisor: Prof. JOONGJAI PANPRANOT, Ph.D. Co-advisor: Assoc. Prof. YUTTANANT BOONYONGMANEERAT, Ph.D.

In this work, Zn/Cu alloy electrocatalysts prepared by electrodeposition of Zn on Cu foil (Zn/Cu) and electrodeposition of Zn and Cu on Cu foil (ZnCu/Cu) in different electrodeposition baths consisting of NaCl bath (Zn/Cu-Na, ZnCu/Cu-Na) and HCl bath (Zn/Cu-H, ZnCu/Cu-H) with deposition times 60 and 200 s were investigated in the electrochemical reduction of CO_2 (CO_2-ERC). As revealed by SEM-EDX and XRD results, the electroplating conditions affected the Zn structure being formed (dendrite or bulky). Under the conditions used, the electrochemical reduction of CO_2 using these electrodes led to the formation of gaseous products including carbon monoxide and hydrogen and liquid products including formate and n-propanol as confirmed by GC and NMR, respectively. Among the catalysts studied, Zn/Cu-Na200 is the best electrocatalyst that produces high CO product with low H_2 at potential -1.6 V vs. Ag/AgCl because of the high coverage of Zn particles on Cu substrate. The catalyst is stable during the 4 hour reaction time although larger dendritic Zn particles were observed after reaction, suggesting the re-depositing of Zn during CO_2 ERC. Zn/Cu-H with bulky structure, on the other hand, led to formate as the outstanding product due probably to the presence of hexagonal close pack (0001) facet that promotes formate production via the reduction of HCOO* intermediate.

Field of Study:	Chemical Engineering	Student's Signature ....
Academic Year:	2019	Advisor's Signature ....
		Co-advisor's Signature ....

ACKNOWLEDGEMENTS

จุฬาลงกรณ์มหาวิทยาลัย

CHULALONGKORN UNIVERSITY

TABLE OF CONTENTS

จุฬาลงกรณ์มหาวิทยาลัย

CHULALONGKORN UNIVERSITY

LIST OF TABLES

LIST OF FIGURES

CHAPTER I

INTRODUCTION

1.1 Introduction

Energy sources in this world more than 80% come from fossil fuels because of easiness and high energy density whereas using fossil fuels cause carbon dioxide in the atmosphere [1]. Carbon dioxide is a major contribution that causes the greenhouse effect, so converting carbon dioxide into useful chemicals is an important issue [2].

Among many methods, electrochemical carbon dioxide reduction on electrocatalysts is a clean process when the process is powered by renewable electricity sources (e.g. sunlight, wind, etc.). Electrochemical carbon dioxide reduction in aqueous electrolytes can produce many carbon-containing products such as carbon monoxide, formic acid/formate, methanol and methane [2].

Among many products, carbon monoxide is interesting because it can be fed as a reactant for the Fischer-Tropsch process to produce hydrocarbon fuels. Moreover, carbon monoxide is a gas product, so it does not need to be extracted from electrolyte as liquid products [2].

There are various catalysts for selective CO production including Au, Ag, and Zn [3]. Among these catalysts, Zn is interesting because Zn is cheaper than Au and Ag [4]. Normally, Zn foil was used as catalyst for electrochemical carbon dioxide reduction but it had still low efficiency and selectivity of CO production [5]. Many literature reported that modified Zn catalyst in different structures such as dendritic structure [6], hexagonal structure [7], and foam structure [8] can improve efficiency and selectivity of CO production but each literature tested modified Zn catalyst in electrochemical carbon dioxide reduction with different parameters. So, it is motivation of this work that compare Zn structures in electrochemical carbon dioxide with same parameters. It was also reported that mixing of Cu and Zn can modified Zn structure [8]. Zn/Cu Alloy catalysts also exhibited higher CO selectivity than pure Cu and pure Zn [9].

In this work, Zn/Cu alloy electrocatalysts were prepared by electrodeposition of Zn on Cu foil (Zn/Cu) and electrodeposition of Zn and Cu on Cu foil (ZnCu/Cu) in various electrodeposition bath consisting of NaCl bath (Zn/Cu-Na, ZnCu/Cu-Na) and HCl bath (Zn/Cu-H, ZnCu/Cu-H) with different deposition times. These catalysts were tested in the electrochemical reduction of CO_2 to CO. The morphology, bulk composition and crystalline structure of these catalysts were investigated by several characterization techniques such as scanning electron microscope-energy dispersive X-ray spectroscopy (SEM-EDX) and X-ray diffraction (XRD).

1.2 Objectives of the Research

1. To study the characteristics and catalytic performances of Zn/Cu alloy electrocatalysts prepared by electrodeposition of Zn on Cu foil (Zn/Cu) and electrodeposition of Zn and Cu on Cu foil (ZnCu/Cu) in various electrodeposition bath consisting of NaCl bath (Zn/Cu-Na, ZnCu/Cu-Na) and HCl bath (Zn/Cu-H, ZnCu/Cu-H) with different deposition times in the electrochemical reduction of CO_2 to CO.

2. To identify appropriate potential and stability of the best Zn/Cu alloy electrocatalyst that gave the highest ratio of CO/H_2 rate from the first objective.

1.3 Scope of the Research

1. Before the electrodeposition and electrolysis experiment, Zn foil (10x25mm^2) and Cu foil (10x25mm^2) were mechanically polished with 800G sandpaper and were rinsed with DI water before drying with N_2.

2. For NaCl bath, Zn/Cu alloy electrocatalysts prepared by electrodeposition of Zn on Cu foil (Zn/Cu) and electrodeposition of Zn and Cu on Cu foil (ZnCu/Cu) in NaCl solution (Zn/Cu-Na, ZnCu/Cu-Na). Various deposition times including 60 s and 200 s. The current density for electrodeposition was set at 20 mA/cm^2. Pt rod was used as counter electrode. After the electrodeposition method, the catalysts were washed with deionized water several times before drying with N_2.

3. For HCl bath, Zn/Cu alloy electrocatalysts prepared by electrodeposition of Zn on Cu foil (Zn/Cu) and electrodeposition of Zn and Cu on Cu foil (ZnCu/Cu) in HCl solution (Zn/Cu-H, ZnCu/Cu-H). Various deposition times including 60 s and 200 s. The current density for electrodeposition was set at 0.3 A/cm^2. Pt rod was used as counter electrode. After the electrodeposition method, the catalysts were washed with deionized water several times before drying with N_2.

4. The catalysts were tested in the electrochemical reduction of CO_2 in an H-type cell at room temperature, ambient pressure, potential -1.6 V vs. Ag/AgCl and inlet CO_2 flow rates 20 mL/min for 70 minutes. The cathodic part and the anodic part of H-type cell were separated by Nafion® 117. Pt foil was used as counter electrode. Ag/AgCl was used as reference electrode.

5. The best one Zn/Cu electrocatalyst that gets the highest CO selectivity was further tested at potential -1.4, -1.8 and -2.0 V vs. Ag/AgCl.

6. The best one Zn/Cu electrocatalyst and appropriate potential that gets the highest CO/H_2 rate ratio was further tested at appropriate potential for 4 h.

7. 20 mL of $KHCO_3$ 0.1 M was used as both catholyte and anolyte. Before the electrolysis experiment, the electrolyte was saturated with 100 mL/min CO_2 gas for 30 minutes.

8. A potentiostat was used for the electrodeposition method and the electrochemical CO_2 reduction experiments.

9. The catalysts were characterized by

    6.1 Scanning electron microscope-energy dispersive X-ray spectroscopy (SEM-EDX)

    6.2 X-ray diffraction (XRD)

CHAPTER II

BACKGROUND AND LITERATURE REVIEWS

2.1 Fundamental of electrochemical reduction of CO_2

The reactions in aqueous solutions vs. NHE at pH 7, 25°C, 1 atm) are given below.

$$CO_2 + H_2O + 2e^- \rightarrow HCOO^- + OH^- \quad (E^\circ = -0.43 \text{ V})$$

$$CO_2 + H_2O + 2e^- \rightarrow CO^- + 2OH^- \quad (E^\circ = -0.52 \text{ V})$$

$$CO_2 + 6H_2O + 6e^- \rightarrow CH_3OH + 6OH^- \quad (E^\circ = -0.38 \text{ V})$$

$$CO_2 + 6H_2O + 8e^- \rightarrow CH_4 + 8OH^- \quad (E^\circ = -0.25 \text{ V})$$

$$2CO_2 + 8H_2O + 12e^- \rightarrow C_2H_4 + 12OH^- \quad (E^\circ = -0.34 \text{ V})$$

$$2CO_2 + 9H_2O + 12e^- \rightarrow C_2H_5OH + 12OH^- \quad (E^\circ = -0.33 \text{ V})$$

$$3CO_2 + 13H_2O + 18e^- \rightarrow C_3H_7OH + 18OH^- \quad (E^\circ = -0.32 \text{ V})$$

$$2H_2O + 2e^- \rightarrow 2OH^- + H_2 \quad (E^\circ = -0.41 \text{ V})$$
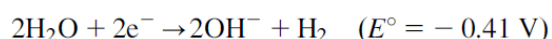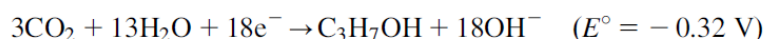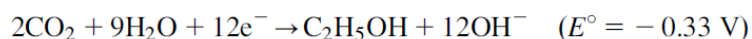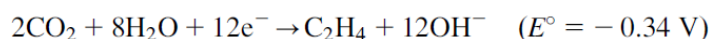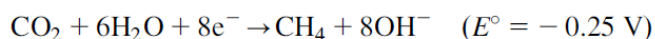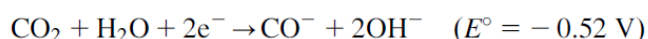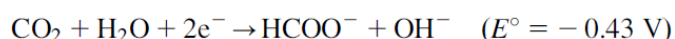
The real potentials are more negative than equilibrium potentials because of single-electron reduction of CO_2 to $CO_2^{\cdot-}$. This reaction requires -1.90 V that is a lot of energy for changing linear molecule of CO_2 into bent radical anion. This step is the first step and the rate determining step (RDS) for reduction of CO_2 [10].

$$CO_2 + e^- \rightarrow CO_2^{\bullet-} \quad (E^\circ = -1.90 \text{ V})$$

Although thermodynamically methane and ethylene occur at less negative potential but this reaction is still limited by kinetics at less negative potential [11]. Increment of negative potential will increase transfer of proton and electron [12].

2.2 Study on electrodes

Various products from electrochemical CO_2 reduction occur depending on electrode and electrolyte that are used in reaction. Various reactions occur on the surface of electrode. The selectivity of product depends on the adsorption strength of substrate [3]. Most studies focus on transition metals beginning in 1985. Hori and Suzuki reported that methane and ethylene are the main products for CO_2 reduction reaction on copper electrode. Many studies have compared the activity of transition metals and found that the product yield of CO_2 reduction reaction depends on the

bind energy of CO with transition metal. Therefore, it is believed that it is an important key for reduction of CO_2. Metals with strong CO binding energy will produce less products form CO_2 reduction reaction because poisoning from CO or other media on the transition metal surface during reaction. Therefore, Hydrogen that occurs from reduction of water is the main product. On the other hand, Metals with weak CO binding energy will produce a lot of CO because CO is released from the metal surface before it can be reduced to other products such as alcohol and hydrocarbons [13].

Mechanism for electrochemical CO_2 reduction on metal surfaces in water show in Figure 1 [10].
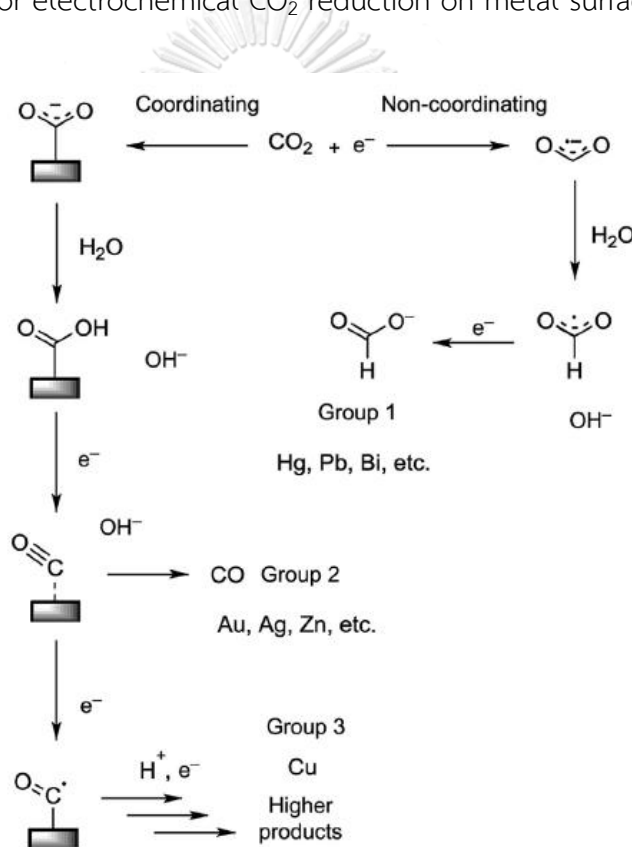
Figure 1 Mechanism for electrochemical CO_2 reduction on metal surfaces in water

CO_2^- will occur in the first step. CO_2^- is high energy and rapidly reacts with water or another CO_2. Subsequent steps occur almost immediately. Metals are classified by binding of CO_2^- intermediate and reducing of CO. Group 1 such as Pb, Hg, In, Sn, Cd, and Tl. These metals are low tendency for binding of CO_2^-. CO_2 reduction reaction occurs through an outer-sphere mechanism and normally produces formate or

formic acid. Group 2 such as Au, Ag, Zn, and Ga. These metals bind CO_2^- intermediate but it cannot further reduce CO. So, CO is the main product. Group 3 such as only Cu. This metal bind CO_2^- and it can further reduce CO into other products such as alcohols and hydrocarbons. Some metals cannot reduce CO_2 readily such as Ni, Fe, Pt, and Ti. These metals strongly bind hydrogen [10]. Table 1-5 show summary of Sn, Au, Ag, Zn and Cu electrodes. Faradaic efficacy (FE) is the selectivity of products [10].

Table 1 Sn based-electrode in electrochemical CO_2 reduction

Electrode	E (V vs. SCE)	Faradaic efficiency			Reference
		CO	Formate	Hydrogen	
Sn foil	-1.7	N/A	95%	N/A	Wu, J. 2012 [14]
Sn plate	-1.85	N/A	>91%	N/A	Lv, W. 2014 [15]
Sn particles deposited over C paper	-1.45	N/A	95%	N/A	Castillo, A. D. 2015 [16]
OE-Sn	-1.85	N/A	85%	N/A	Zhang, R. 2015 [17]
Sn/Cu	-1.4	N/A	>91%	N/A	Zhoa, C. 2016 [18]
Sn/f-Cu	-1.85	N/A	83.5%	N/A	Wang, Y. 2016 [19]
SnO_2/CA GDE	-1.65	N/A	76%	~24%	Yu, J. 2017 [20]
SnS_2/rGO	-1.45	~6%	84.5%	~17%	Li, F. 2017 [21]
Sn plate	-1.8	N/A	40.2%	N/A	Jiang, H. 2018 [22]
mesoporous SnO_2	-1.44	~37%	~40%	~23%	Ge, H. 2018 [23]
Ag-Sn	-1.47	~10%	85%	~5%	Wang, S. 2019 [24]
Sn metal	-2.04	N/A	80%	N/A	Rasul, S. 2019 [25]
SnO_2/γ-Al_2O_3/CPF	-2.05	N/A	65%	N/A	Kim, Y, E. 2019 [26]
SnO_2 –NCs loaded C fiber	-1.59	~13%	~73%	~8%	Yang, H. 2019 [27]
Cu-Sn	-1.24	>90%	N/A	<8%	Sarfraz, S. 2016 [28]
Cu-Sn foam	-1.44	94%	~1%	~5%	Zeng, J. 2018 [29]

Table 2 Au based-electrode in electrochemical CO_2 reduction

Electrode	E (V vs. SCE)	Faradaic efficiency			Reference
		CO	Formate	Hydrogen	
Oxide-derived Au	-1.02	>96%	~1%	N/A	Chen, Y. 2012 [1]
Gold sheet	-2.8	93%	N/A	N/A	Li, Q. 2017 [30]
Au foil	-3.14	92%	N/A	~5%	Shi, J. 2017 [31]
Au/Cu	-1.64	58%	1%	41%	Kim, J. 2017 [32]
PF-Au-75	-1.27	90.5%	N/A	~10%	Chen, C. 2017 [33]
Au foil	-1.32	97.01%	~3%	~5%	Cave, E. R. 2017 [34]
Au foil	-2.7	92%	N/A	8%	Shen, F. 2018 [35]
Au on hydrophobic carbon substrate	-1.37	94%	N/A	~3%	Park, G. 2019 [36]
Gold disc	-1.35	74%	N/A	~26%	Ahangari, H. T. 2019 [37]
Au/Cu foam	-1.4	41.3%	N/A	N/A	Lee, H. 2017 [38]
PVA-Au/C	-1.25	97%	N/A	N/A	Ma, L. 2019 [39]

Table 3 Ag based-electrode in electrochemical CO_2 reduction

Electrode	E (V vs. SCE)	Faradaic efficiency			Reference
		CO	Formate	Hydrogen	
Silver foil	-1.74	>90%	~3%	~10%	Hatsukade, T. 2014 [12]
Ag GDE	-3.05	>80%	N/A	<20%	Kim, B. 2015 [40]
Ag_{100} dendrite	-1.7	64.6%	N/A	~13%	Choi, J. 2016 [2]
$Ag_{66.0}In_{34.0}$	-1.04	65.3%	N/A	~30%	Park, H. 2017 [41]
Ag/Cu	-1.5	60.81%	N/A	~22%	Ham, Y. S. 2017 [42]
Dendritic Ag/CP	-1.5	80.7%	N/A	~15%	Ham, Y. S. 2018 [43]
Ag foil	-2.7	85%	N/A	15%	Shen, F. 2018 [35]
Ag/In/Cu foam	-1.2	77.4%	N/A	~19%	Lee, H. 2018 [44]
Ag foam	-1.43 to -1.73	>94%	N/A	~1%	Rudnev, A. V. 2019 [45]

Table 4 Zn based-electrode in electrochemical CO_2 reduction

Electrode	E (V vs. SCE)	Faradaic efficiency			Reference
		CO	Formate	Hydrogen	
RE-Zn	-1.77	95.3%	N/A	N/A	Nguyen, D. L. T. 2017 [4]
Porous network Zinc	1.77	~80%	~10%	~10%	Lu, Y. 2018 [46]
Zn foil	-2.7	90%	N/A	5.2%	Shen, F. 2018 [35]
Multilayered Zn nanosheets	-1.8	86%	N/A	~14%	Zhang, T. 2018 [47]
Porous Zn	-1.43	81%	N/A	~11%	Morimoto, M. 2018 [48]
ZnS/Zn	-2.8	92%	N/A	5.2%	Zhen, J. 2019 [49]

Table 5 Cu based-electrode in electrochemical CO_2 reduction

Electrode	E (V vs. SCE)	Faradaic efficiency								Reference
		CO	Formate	Hydrogen	Methane	Ethylene	Ethanol	n-Propanol	Allyl alcohol	
Copper foil	-1.69	~1%	~1%	~22%	~25%	~27%	~10%	~2.5%	~1%	Kuhl, K. P. 2012 [50]
Cu oxide NNs	-1.84	N/A	~19%	~17%	~14%	~6%	N/A	N/A	N/A	XIE, J. 2015 [51]

2.3 Modification of morphology of Zn electrocatalysts

Table 6 Modification of morphology of Zn electrocatalysts in electrochemical CO_2 reduction

Researcher	Electrode name	Catalyst preparation	Faradaic efficiency
Quan, F. et al.	nanoscale Zn	Zn foil was anodized at 0.3 mA/cm^2 for 90 min in zincate-saturated solution. Then, Zn	CO : 57% at -1.6 V

(2015) [5]		foil was activated at 5 mA/cm^2 for 5 min in 0.2 M Na$_3$PO$_4$. Then, Zn foil was reduced at -1.3 V vs. SCE for 30 min in 0.5 M NaHCO$_3$. in 50% H$_3$PO$_4$ for 2 min at 2.1 V.	vs. SCE
Rosen, J. et al. (2015) [6]	Zn dendrite	Zn foil was polished with sand paper. Then, Zn foil was sonicated in acetone and water. Zn foil was used as working electrode for deposition. Current density was applied at -1 A/cm^2 for 60 s. ZnO powder was dissolved in 6 M KOH and was used as supporting electrolyte.	CO : 79% at -1.1 V vs. RHE
Won, D.H. et al. (2016) [7]	Hexagonal Zn	Zn foil was polished with sand paper. Then, Zn foil was cleaned with ethanol, acetone, and DI. Zn foil was used as working electrode for deposition. Current density was applied at multi-step potentials for 3 s each of −2 and −2.5 V vs. SCE with 30 cycles. SCE was used as reference electrode. Pt coil was used as counter electrode. Supporting electrolyte include 0.05 M ZnCl$_2$.	CO : 85% at -0.95 V vs. RHE
Moreno-García, P. et al. (2018) [8]	Foam Zn	Cu foil (0.8x20 mm^2) was electropolished in 50% H$_3$PO$_4$ for 2 min at 2.1 V. Then, Cu foil was rinsed by Milli-Q water and sonicated in ethanol for 15 min. Area for deposition was 1 cm^2. Cu foil was used as working electrode for deposition. Current density was applied at -3 A/cm^2 for 20 s. Ag/AgCl was used as reference electrode. Zn foil was used as counter electrode. Supporting	CO : 90% at -0.95 V vs. RHE

		electrolyte include 1.5M H_2SO_4, 0.203M $ZnSO_4$ and 0.006 M $CuSO_4$.	

Quan, F. et al. (2015) [5] studied nanoscale Zn that was prepared by a facile electrochemical strategy. CO faradaic efficiency was 57% at -1.6 V vs. SCE for $NaHCO_3$ solution. Highest CO faradaic efficiency was 93% at -1.6 V vs. SCE for NaCl solution. The high conversion efficiency is the result of the nano-size of the catalyst. Nanoscale Zn has resistance to deactivation during electrolysis.

Rosen, J. et al. (2015) [6] studied Zn dendrite by electrodeposition method. The results showed highest CO faradaic efficiency 79% at -1.1 V vs. RHE. Because Zn dendrite has a higher density of stepped sites that suppress hydrogen evolution.

Won, D.H. et al. (2016) [7] studied Hexagonal Zn by electrodeposition method. The results showed highest CO faradaic efficiency 85% at -0.95 V vs. RHE. Because Zn(101) facet was developed for Hexagonal Zn and Zn(101) facet has low reduction potential for CO_2 reduction to CO.

Moreno-García, P. et al. (2018) [8] studied Zn–Cu alloys by electrodeposition method with different ratio of Zn ion and Cu ion in bath. The results showed $Zn_{94}Cu_6$ (ratio Zn 30 : Cu 1) was the best in this work. Highest CO faradaic efficiency 90% at -0.95 V vs. reversible hydrogen electrode because of high density of low-coordinated active sites and more Zn(101) than Zn(002).

2.4 Electrodeposition of Zn/Cu alloy electrocatalysts

Electrodeposition was performed in electrolysis cell including an electrolytic bath, an anode (the positive electrode), a cathode (the negative electrode), a current source and an ampere/volt meter. Reduction reaction occurs at cathode. Oxidation reaction occurs at anode. Cathode is substrate that is deposited by metal (M). Anode is soluble or inert [52].

$$\text{Reduction reaction:} \quad M^{z+} + ne^- \rightarrow M$$

$$\text{Oxidation reaction for soluble anode:} \quad M \rightarrow M^{z+} + ne^-$$

$$\text{Oxidation reaction for inert anode:} \quad H_2O \rightarrow 2H^+ + 1/2\,O_2 \uparrow + 2\,e^-$$
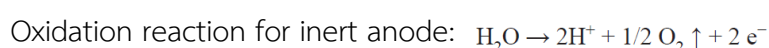
Figure 2 show schematic representation of steps in the cathodic deposition of metals in simple salt solutions. Metal ion in bulk solution is a form of hydrated ions $M(H_2O)_x^{Z+}$, where x is number of water molecules. Hydrated ions are transported to cathode surface. Alignment of water molecules occurs in diffusion layer and is removed in Helmholtz layer. Then, adsorption of ions occurs at cathode surface (adatoms). Then, surface diffusion and the incorporation of adatoms occur into the crystal lattice [52].
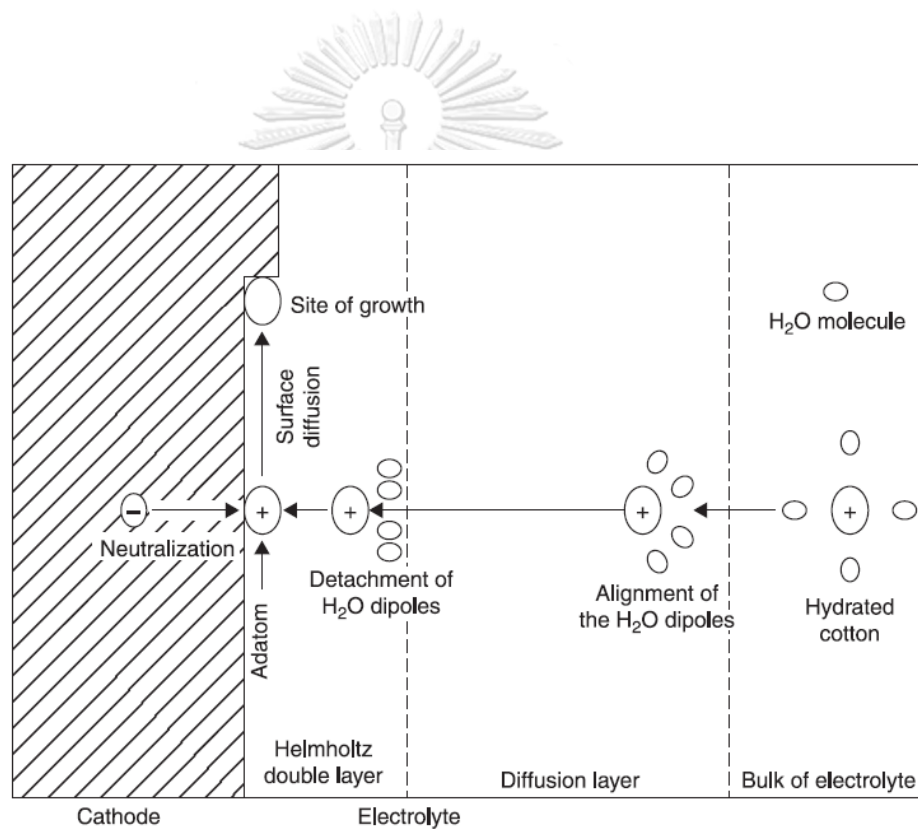
Figure 2 Schematic representation of steps in the cathodic deposition of metals.

The quantity of metal deposited (W) on cathode surface is calculated from the electrochemical equivalent of the metal (z_c) and the product of quantity of total coulombs passed (Q_c).

$$Q_c = \int I\, \partial t$$

$$z_c = M_w / nF$$

$$W = \int I\, \partial t\, M_w / nF$$

Where I is applied current, t is times, M_w is molecular weight of metal, F is faradaic constant and n is number of electron [52].

Table 7 Zn/Cu alloy electrocatalysts by electrodeposition

Researcher	Electrode name	Catalyst preparation	Faradaic efficiency
Katah, A. et al. (1994) [53]	pure Zn	Gold flag electrode (1.5x1.5 cm^2) was used as working electrode for electroplating with a 10 C charge. Current density was applied at 200 A/m^2. Bath compositions include 150 g/dm^3 $ZnCl_2$ and 25 g/dm^3 NaCl (pH3.7).	CO : 30% at -1.50 V vs. SHE
	Cu-Zn alloy	Gold flag electrode (1.5x1.5 cm^2) was used as working electrode for electroplating with a 10 C charge. Current density was applied at 222 A/m^2. Bath compositions include 17 g/dm^3 $Cu(CN)_2$, 60 g/dm^3 $Zn(CN)_2$, 80 g/dm^3 KCN and 60 g/dm^3 KOH.	CO : 80% at -1.50 V vs. SHE
Keerthiga, G. et al. (2017) [9]	Cu/Zn-A	Zn sheet was polished with sand paper and then used as counter electrode. Potential for deposition was applied at -0.3 V vs. platinum for 15 min. Cu was polished with sand paper and immersed in 1 M H_3PO_4 and 1 M H_2SO_4	CH_4 : 15% C_2H_6 : 10% at -1.8 V vs. NHE

		for 15 min. Then, Cu was washed with acetone and DI before drying with N_2. Then, Cu was used as working electrode. Platinum was used as reference electrode. 0.6 M sodium zincate was used as electrolytic solution.	
	Cu/Zn-B	Zn sheet was polished with sand paper and then used as counter electrode. Potential for deposition was applied at -0.3 V vs. platinum for 15 min. Cu was polished with sand paper and immersed in 1 M H_3PO_4 and 1 M H_2SO_4 for 15 min. Then, Cu was washed with acetone and DI before drying with N_2. Then, Cu was used as working electrode. Platinum was used as reference electrode. 6 M sodium zincate was used as electrolytic solution.	CH_4 : 52% C_2H_6 : 25% at -1.6 V vs. NHE

Katah, A. et al. (1994) [53] studied Cu-Zn alloys electrodes by electroplating with different composition of Zn ion and Cu ion in bath. The results showed various crystals of Zn and Cu when deposition with different composition bath. Selectivity and reactivity of CO were excellent for Cu_5Zn_8 crystals.

Keerthiga, G. et al. (2017) [9] studied zinc-modified copper electrodes by electrodeposition method. The bath concentration of Zn was varied during low concentration (low deposit of Zn on Cu, Cu/Zn-A) and high concentration (high deposit of Zn on Cu, Cu/Zn-B). The results showed Cu/Zn-B got conversion efficiency more than Cu/Zn-A. Descending order of CH_4 faradaic efficiency was shown as: Cu/Zn-B (52%) > Cu (23%) > Zn (7%). Hydrogen was suppressed for Cu/Zn-B (8%) when compared with bare Cu (68%).

CHARPTER III

MATERIALS AND METHODS

3.1 Materials

Table 8 Chemicals used as precursors and electrolyte.

Chemicals	Formular	Suppliers
Zinc chloride	$ZnCl_2$	Ajax Finechem Pty Ltd
Copper(II) chloride dihydrate	$CuCl_2 \cdot 2H_2O$	Aldrich Chemical Ltd
Potassium hydrogen carbonate	$KHCO_3$	Acros Organics
Hydrochloric acid	HCl	Merck Ltd
Sodium chloride	$NaCl$	Sigma-Aldrich

Table 9 Metals used as electrodes in electrodeposition method and electrochemical reduction of CO_2

Electrodes	Suppliers
Copper foil (0.1mm thick, 99.9999%)	Alfa Aesar
Zinc foil (0.1mm thick, 99.994%)	Alfa Aesar
Platinum foil (0.1mm thick, 99.997%)	Alfa Aesar
Platinum rod (Length 76mm, Diameter 2mm)	Metrohm

3.2 Catalyst preparation

3.2.1 Preparation of zinc foil and copper foil

Before the electrodeposition and electrolysis experiment, Zn foil ($10x25mm^2$) and Cu foil ($10x25mm^2$) were mechanically polished with 800G sandpaper and were rinsed with DI water before drying with N_2.
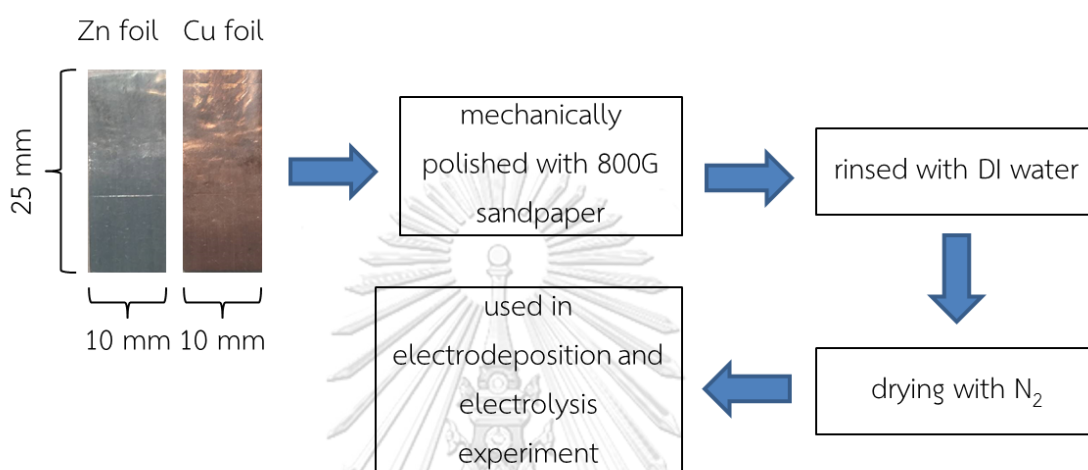
Figure 3 Schematic of preparation of zinc foil and copper foil

3.2.2 Preparation of Zn/Cu-Na and ZnCu/Cu-Na in NaCl bath

The Zn/Cu-Na catalysts were prepared on a Cu foil substrate using an electrodeposition method. $ZnCl_2$ was used as the Zn precursors with NaCl. The concentrations of $ZnCl_2$ and NaCl was fixed at 0.05 M. Various deposition times including 60 s and 200 s (Zn/Cu-Na60, Zn/Cu-Na200). The ZnCu/Cu-Na catalysts were prepared on a Cu foil substrate using an electrodeposition method. $ZnCl_2$ and $CuCl_2$ were used as the Zn and Cu precursors with NaCl. The concentrations of $ZnCl_2$ and NaCl were fixed at 0.05 M. The concentration of $CuCl_2$ was fixed at 0.0015 M. Various deposition times including 60 s and 200 s (ZnCu/Cu-Na60, ZnCu/Cu-Na200). The current for electrodeposition was set at 20 mA/cm^2. Pt rod was used as counter electrode. After the electrodeposition method, these catalysts were washed with deionized water several times before drying with N_2.

Deposition current : 20 mA/cm^2
Deposition times : 60s, 200s
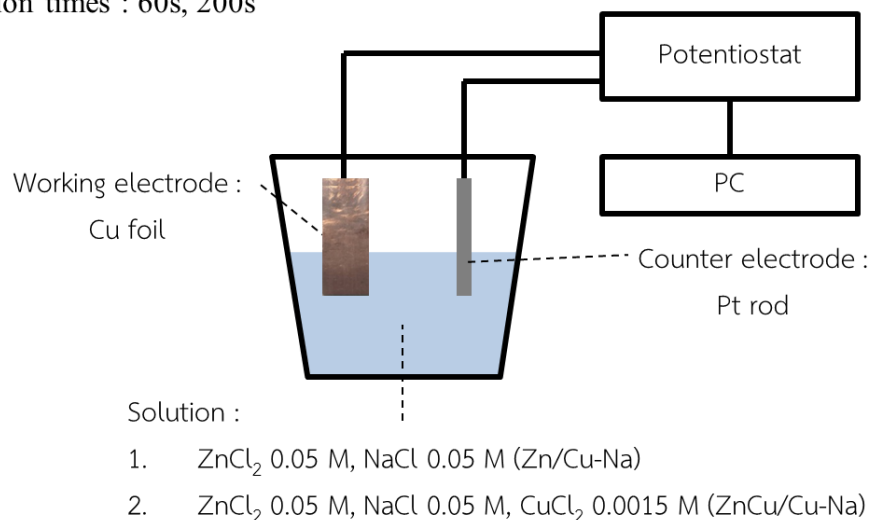
Figure 4 Schematic of preparation of Zn/Cu-Na and ZnCu/Cu-Na in NaCl bath

3.2.3 Preparation of Zn/Cu-H and ZnCu/Cu-H in HCl bath

The Zn/Cu-H catalysts were prepared on a Cu foil substrate using an electrodeposition method. $ZnCl_2$ was used as the Zn precursors with HCl. The concentrations of $ZnCl_2$ and HCl were fixed at 0.2 M and 1.5 M, respectively. Various deposition times including 60 s, and 200 s (Zn/Cu-H60, Zn/Cu-H200). The ZnCu/Cu-H catalysts were prepared on a Cu foil substrate using an electrodeposition method. $ZnCl_2$ and $CuCl_2$ were used as the Zn and Cu precursors with HCl. The concentrations of $ZnCl_2$ and HCl were fixed at 0.2 M and 1.5 M, respectively. The concentration of $CuCl_2$ was fixed at 0.006 M. Various deposition times including 60 s, and 200 s (ZnCu/Cu-H60, ZnCu/Cu-H200). The current for electrodeposition was set at 0.3 A/cm^2. Pt rod was used as counter electrode. After the electrodeposition method, these catalysts were washed with deionized water several times before drying with N_2.

Deposition current : 0.3 A/cm^2
Deposition times : 60s, 200s
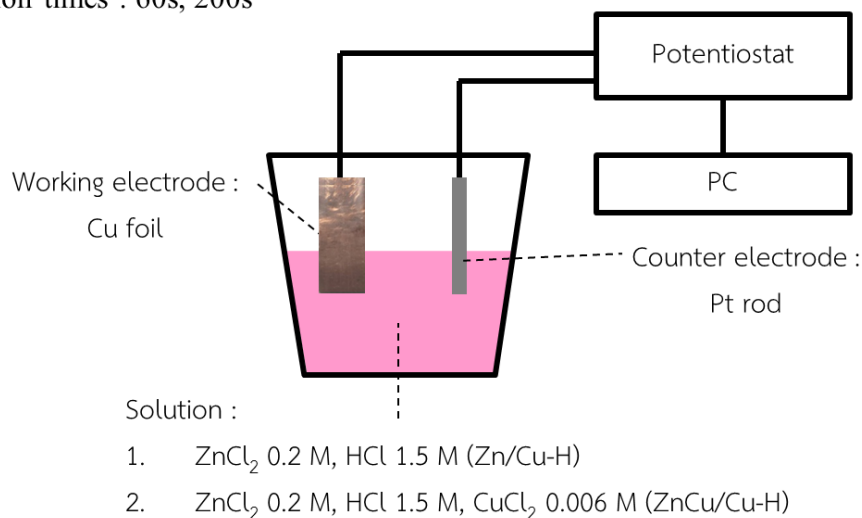
Figure 5 Schematic of preparation of Zn/Cu-H and ZnCu/Cu-H in HCl bath

3.3 Catalyst Characterization

3.3.1 Scanning electron microscope-energy dispersive X-ray spectroscopy (SEM-EDX)

Zn foil, Cu foil, Zn/Cu-Na60, Zn/Cu-Na200, ZnCu/Cu-Na60, ZnCu/Cu-Na200, Zn/Cu-H60, Zn/Cu-H200, ZnCu/Cu-H60, and ZnCu/Cu-H200 were characterized by scanning electron microscopy (SEM) of Hitachi mode S-3400N and energy dispersive X-ray spectroscopy (EDX) to investigate the morphology of the surface and the bulk composition, respectively.

3.3.2 X-ray diffraction (XRD)

The X-ray diffraction (XRD) pattern of electrocatalyst samples were recorded in the 2θ range 20°-80° (scan rate = 0.5 sec/step) using a Siemens D5000 diffractometer using nickel filtered Cu K$_\alpha$ radiation.

3.4 Electrochemical CO$_2$ reduction

Electrochemical reduction of CO$_2$ was performed in an H-type cell, and all experiments were performed at room temperature and ambient pressure. The cathodic part and the anodic part were separated by Nafion® 117. All the experiments were carried out in a three-electrode cell system. Zn foil, Cu foil, Zn/Cu-

Na60, Zn/Cu-Na200, ZnCu/Cu-Na60, ZnCu/Cu-Na200, Zn/Cu-H60, Zn/Cu-H200, ZnCu/Cu-H60, and ZnCu/Cu-H200 were used as the working electrodes which were immersed in electrolyte solution with a geometrical area of 1 cm^2. Silver/silver chloride electrode (Ag/AgCl) was used as the reference electrode. Platinum foil was used as the counter electrode. $KHCO_3$ 0.1 M 20 mL was used both as catholyte and anolyte. The electrolyte was saturated with 100 mL/min CO_2 gas for 30 minutes. CO_2 flow rate of 20 mL/min was performed during reaction. A potentiostat was used for all the electrochemical CO_2 reduction experiments. Potential was used at -1.6 V vs. Ag/AgCl. Electrolysis was performed for 70 minutes. The gas chromatography system with a thermal conductivity detector (TCD), which was used to analyze H_2 and CO. Liquid phase products were identified and quantified using NMR. The best one Zn/Cu alloy electrocatalyst that gets the highest CO selectivity was further tested at potential -1.4, -1.8 and -2.0 V vs. Ag/AgCl. For stability test, the best one Zn/Cu alloy electrocatalyst and appropriate potential that gets the highest CO/H_2 rate ratio was further tested at appropriate potential for 4 h.
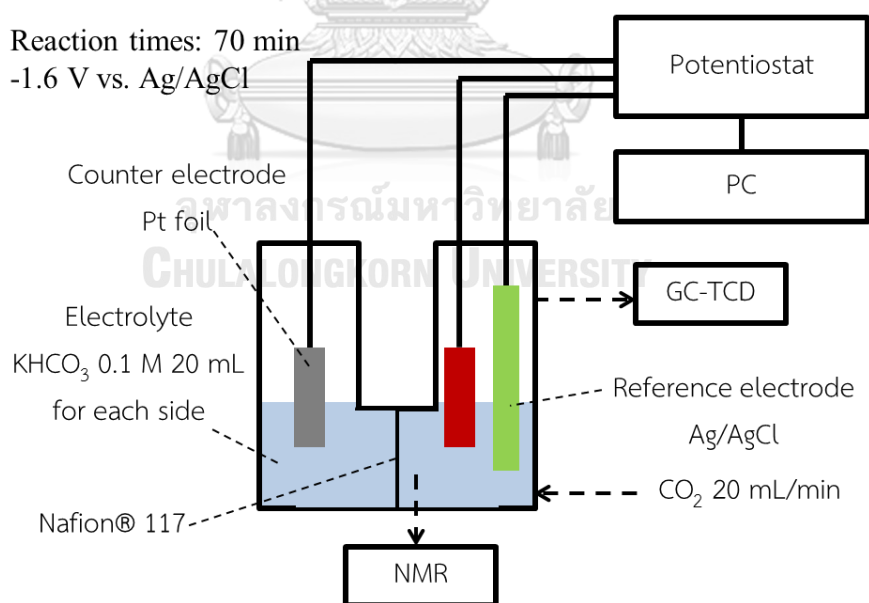
Figure 6 Schematic of electrochemical CO_2 reduction.

Table 10 The operating conditions of gas chromatograph with a thermal conductivity detector

Gas chromatography (Shimadzu GC-2014)	Conditions
Detector	TCD
Column information	Shincarbon ST(50/80)
Carrier gas	Helium (99.999%)
Injector temperature	180°C
Column initial temperature	40°C, Hold time 5 min
Column temperature rate	10°C/min
Column final temperature	200°C
Detector temperature	170°C
Total time analysis	21 min

3.5 Research methodology

Part I. To study the characteristics and catalytic performances of Zn/Cu alloy electrocatalysts prepared by electrodeposition of Zn on Cu foil (Zn/Cu) and electrodeposition of Zn and Cu on Cu foil (ZnCu/Cu) in various electrodeposition bath consisting of NaCl bath (Zn/Cu-Na, ZnCu/Cu-Na) and HCl bath (Zn/Cu-H, ZnCu/Cu-H) with different deposition times in the electrochemical reduction of CO_2 to CO.

Zn/Cu-Na were prepared by electrodeposition of Zn on Cu foil in NaCl bath with deposition times 60 s and 200 s (Zn/Cu-Na60, Zn/Cu-Na200). ZnCu/Cu-Na were prepared by electrodeposition of Zn and Cu on Cu foil in NaCl bath with deposition times 60 s and 200 s (ZnCu/Cu-Na60, ZnCu/Cu-Na200).

Zn/Cu-H were prepared by electrodeposition of Zn on Cu foil in HCl bath with deposition times 60 s, and 200 s (Zn/Cu-H60, Zn/Cu-H200). ZnCu/Cu-H were prepared by electrodeposition of Zn and Cu on Cu foil in HCl bath with deposition times 60 s and 200 s (ZnCu/Cu-H60, ZnCu/Cu-H200).

Catalyst test in the electrochemical reduction of CO_2 at potential -1.6 V vs. Ag/AgCl for 70 min.

GC-TCD, NMR analysis and data

Catalyst characterizations
✔ SEM-EDX
✔ XRD

Discussions and conclusions

Part II. To identify appropriate potential and stability of the best one Zn/Cu alloy electrocatalyst that gets the highest CO/H$_2$ rate ratio from Part I.

The best one Zn/Cu electrocatalyst that gets the highest CO/H$_2$ rate ratio from Part I was further tested at potential -1.4, -1.8 and -2.0 V vs. Ag/AgCl.

For stability test, the best one Zn/Cu electrocatalyst and appropriate potential that gets the highest CO/H$_2$ rate ratio was further tested at appropriate potential for 4 h.

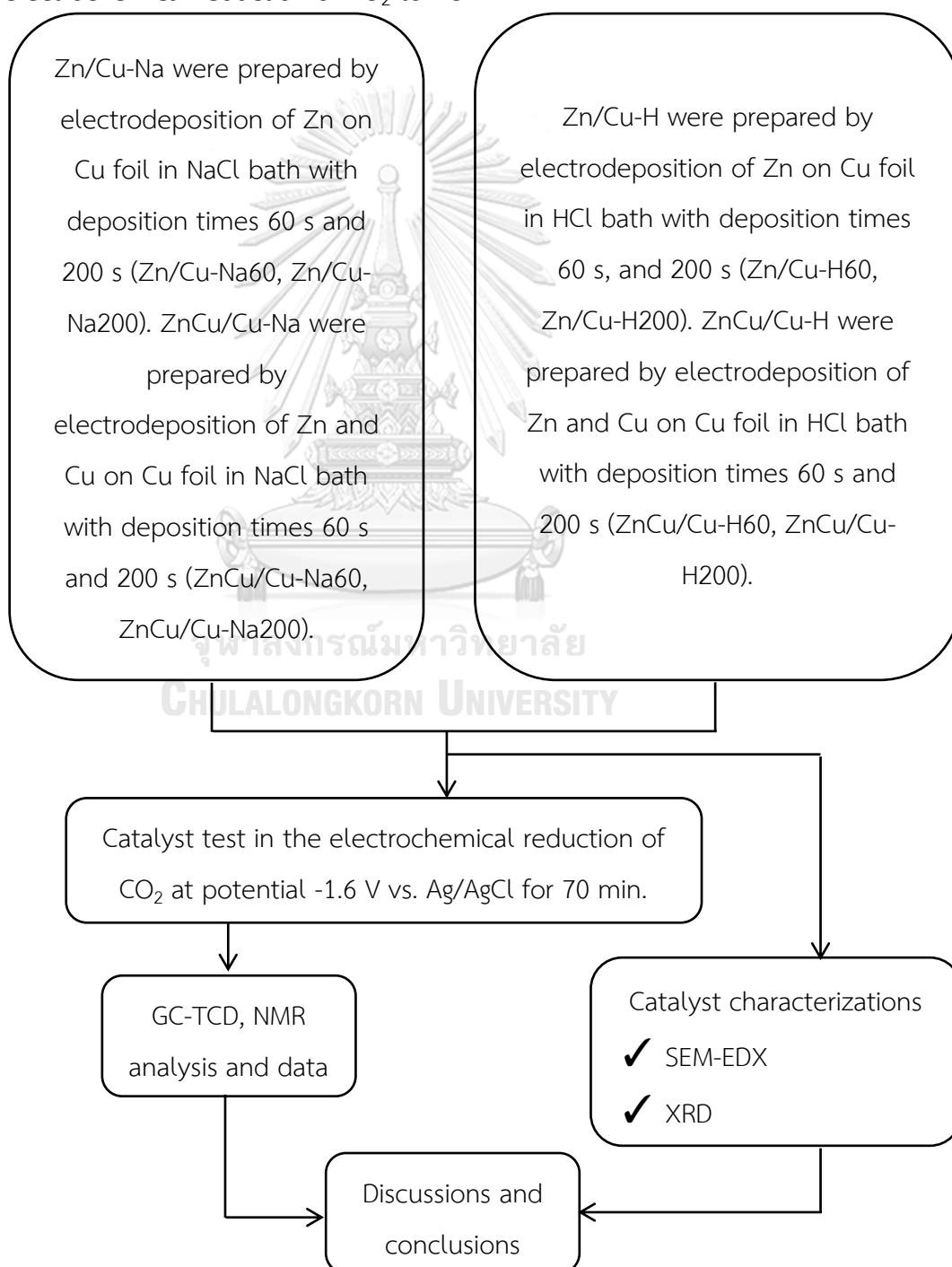GC-TCD, NMR analysis and data

GC-TCD analysis and data

Catalyst characterizations
✓ SEM-EDX

Discussions and conclusions

CHARPTER IV

RESULTS AND DISCUSSION

Part I. To study the characteristics and catalytic performances of Zn/Cu alloy electrocatalysts prepared by electrodeposition of Zn on Cu foil (Zn/Cu) and electrodeposition of Zn and Cu on Cu foil (ZnCu/Cu) in various electrodeposition bath consisting of NaCl bath (Zn/Cu-Na, ZnCu/Cu-Na) and HCl bath (Zn/Cu-H, ZnCu/Cu-H) with different deposition times in the electrochemical reduction of CO_2 to CO.

4.1 Characterization of Zn/Cu alloy electrocatalysts with different deposition times

4.1.1 X-ray diffraction (XRD)

The samples were examined by X-ray diffraction, and Figure 7 showed the XRD patterns of Zn foil, Cu foil, Zn/Cu-Na60, Zn/Cu-Na200, ZnCu/Cu-Na60, ZnCu/Cu-Na200, Zn/Cu-H60, Zn/Cu-H200, ZnCu/Cu-H60, and ZnCu/Cu-H200. All electrocatalysts except Zn foil showed the XRD characteristic peak around 50.1$^{\text{o}}$ that related to Cu(200) facet [9]. Cu(200) facet occurs from Cu substrate that is used for electrodeposition method. Cu(200) intensity of Cu foil is higher than deposited electrocatalysts. Decreasing Cu(200) intensity of deposited electrocatalysts is affected from electrodeposition Zn on Cu foil. In the part of Zn/Cu-Na, ZnCu/Cu-Na, Zn/Cu-H and ZnCu/Cu-H, the Cu(200) intensity decreased when increasing deposition time from 60 s to 200 s because Cu substrate was deposited by a lot of Zn. When comparing between Zn/Cu-Na and ZnCu/Cu-Na, Cu(200) intensity of ZnCu/Cu-Na is higher than Zn/Cu-Na this was probably due to the effect of Cu that is deposited on Cu foil affecting the increasing of Cu(200) intensity. However, when comparingZn/Cu-H and ZnCu/Cu-H, intensity of the Cu(200) was not affected by the addition of Cu Maybe because of the changes in morphology. When compared electrocatalysts from NaCl bath with HCl bath, Cu(200) intensity of electrocatalysts from HCl bath is lower than NaCl bath because of the higher $ZnCl_2$ concentration and deposited

current for HCl bath. Thus, electrocatalysts from HCl bath resulted in a lot of Zn on Cu foil. Figure 8 shows the enlarged XRD patterns of Zn foil, Cu foil, Zn/Cu-Na60, Zn/Cu-Na200, ZnCu/Cu-Na60, ZnCu/Cu-Na200, Zn/Cu-H60, Zn/Cu-H200, ZnCu/Cu-H60 and ZnCu/Cu-H200. The XRD pattern of Zn foil and Cu foil (Figure 8a and 8b) corresponded to Zn and Cu by their reported diffraction peaks (Cu: JCPDS 04-0836, Zn: JCPDS 00-004-0831). The XRD patterns of deposited electrocatalysts match well with diffraction peaks of Zn foil and Cu foil. Among the XRD patterns of deposited electrocatalysts, Cu_4Zn phase was detected on the XRD patterns of Zn/Cu-H60, Zn/Cu-H200, ZnCu/Cu-H60 and ZnCu/Cu-H200 [8]. The intensity of Zn facet increased with increasing deposition time from 60 s to 200 s. However, for ZnCu/Cu-H60, the Zn(002) intensity is relatively high and the Zn(002) intensity of ZnCu/Cu-H60 decreased with increasing deposition time from 60 s to 200 s (ZnCu/Cu-H200).
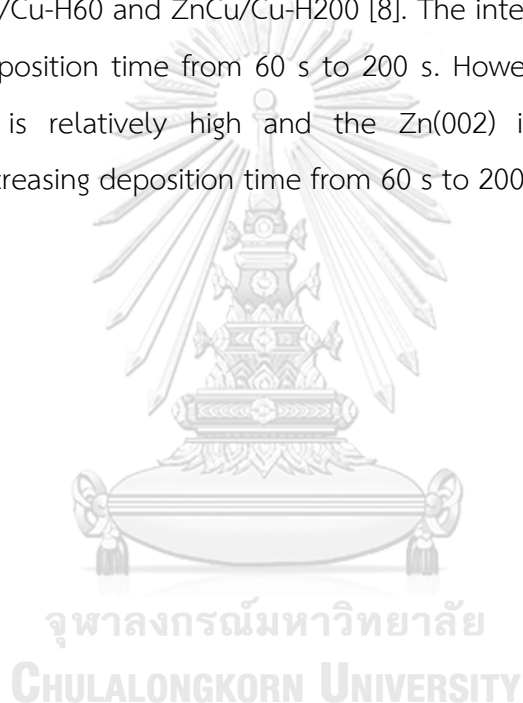
Figure 7 XRD pattern of (a) Zn foil, (b) Cu foil, (c) Zn/Cu-Na60, (d) Zn/Cu-Na200, (e) ZnCu/Cu-Na60, (f) ZnCu/Cu-Na200, (g) Zn/Cu-H60, (h) Zn/Cu-H200, (i) ZnCu/Cu-H60 and (j) ZnCu/Cu-H200

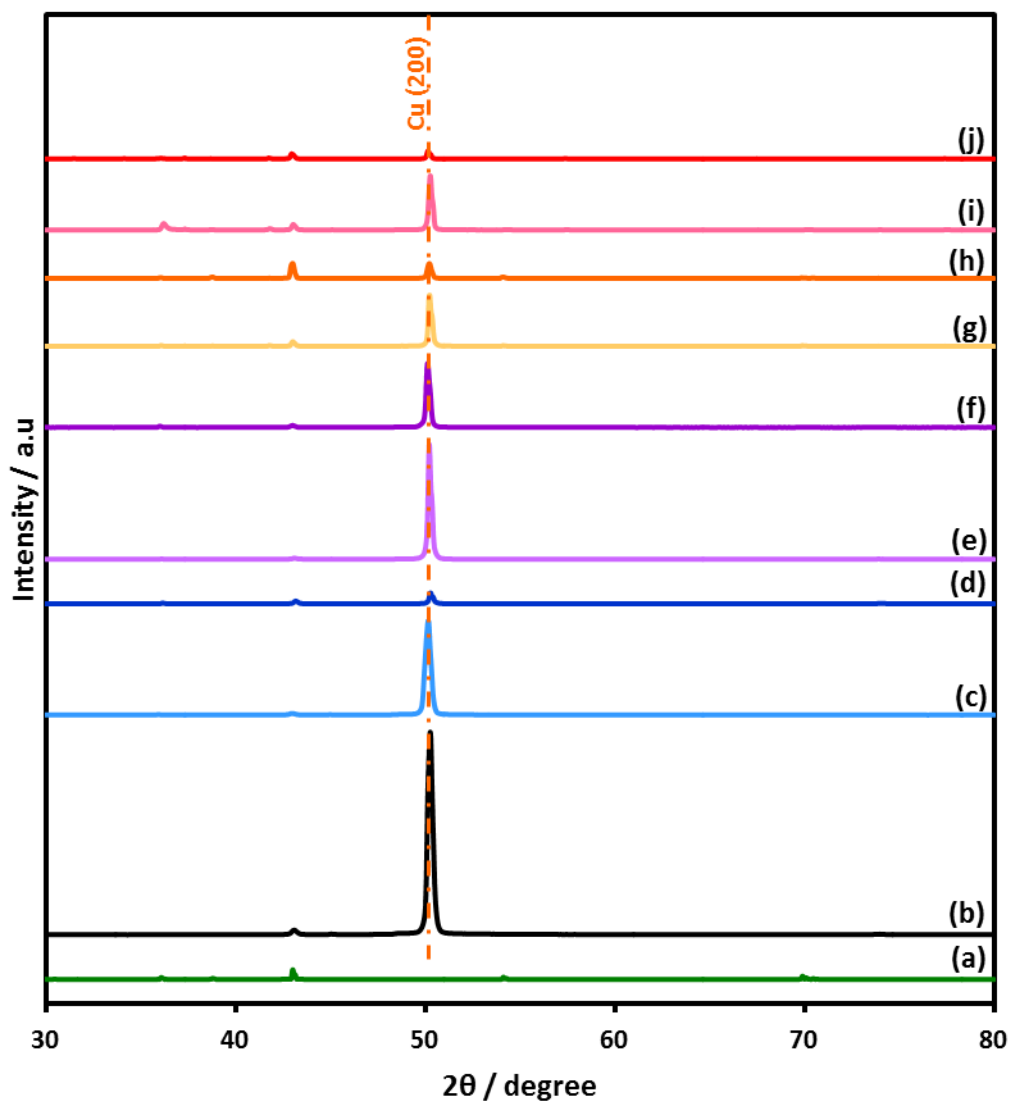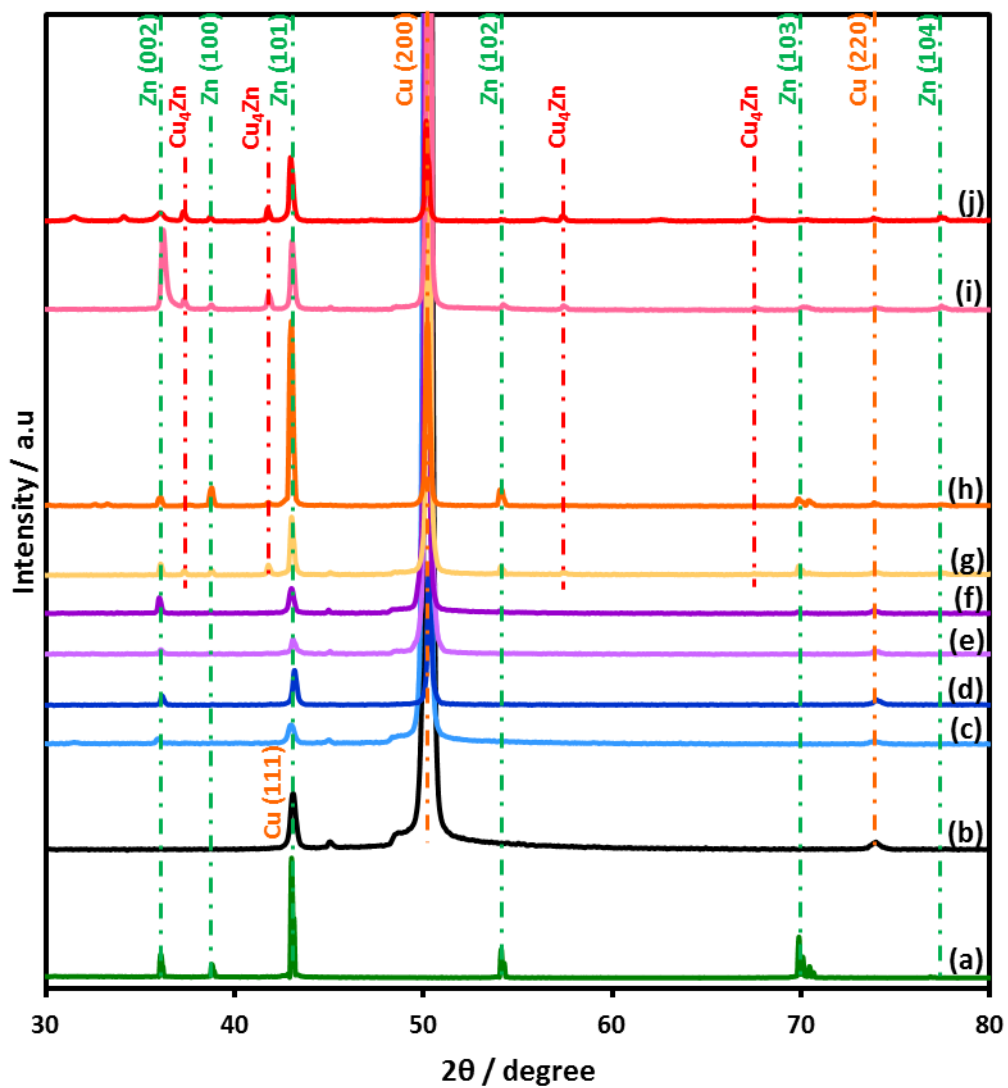Figure 8 Enlarged XRD pattern of (a) Zn foil, (b) Cu foil, (c) Zn/Cu-Na60, (d) Zn/Cu-Na200, (e) ZnCu/Cu-Na60, (f) ZnCu/Cu-Na200, (g) Zn/Cu-H60, (h) Zn/Cu-H200, (i) ZnCu/Cu-H60 and (j) ZnCu/Cu-H200

4.1.2 Scanning electron microscope-energy dispersive X-ray spectroscopy (SEM-EDX)

Table 11 Percent by weight of deposited electrocatalysts

Entry	Electrocatalyst	Percent by weight	
		Zn (%)	Cu (%)
1	Zn/Cu-Na60	74.9	25.1
2	Zn/Cu-Na200	92.9	7.1
3	ZnCu/Cu-Na60	72.5	27.5
4	ZnCu/Cu-Na200	93.1	6.9
5	Zn/Cu-H60	96.0	4.0
6	Zn/Cu-H200	98.1	1.9
7	ZnCu/Cu-H60	86.1	13.9
8	ZnCu/Cu-H200	88.8	11.2

Table 11 shows the percent by weight of Cu and Zn on the deposited electrocatalysts. All deposited electrocatalysts, percent by weight of Zn increased with increasing deposition time from 60 s to 200 s. For electrodeposition using HCl bath, when Cu ion was added, higher percent by weight of Cu was observed. This was not the case for electrodeposition using NaCl bath that there was no significant change in percent by weight of Cu upon addition of Cu ion during electrodeposition, due probably to the low concentration of $CuCl_2$ in deposited bath.

The scanning electron microscopic images of Zn foil, Cu foil, Zn/Cu-Na60, Zn/Cu-Na200, ZnCu/Cu-Na60, ZnCu/Cu-Na200, Zn/Cu-H60, Zn/Cu-H200, ZnCu/Cu-H60 and ZnCu/Cu-H200 are shown in Figure 9. Figure 9a corresponds to Zn foil and Figure 9b corresponds to Cu foil, showing a rock-like surface with some streaks, presumably left by the mechanical polishing pretreatment. As shown in Figure 9c and 9d, Zn/Cu-Na60 and Zn/Cu-Na200 have dendritic structures. Because deposition rate of Zn is very high for concentration of $ZnCl_2$ (0.05 M), the regions of electrocatalyst surface have low concentration of Zn ion. Thus, It forced the dendritic structures to grow outward toward high concentration regions of Zn ion [6].

The morphology of Zn/Cu-Na60 and Zn/Cu-Na200 are similar. Thus, it can be concluded that deposition time does not affect the morphology of Zn/Cu-Na. When adding Cu ion during the electroplating, dendritic structures were also observed as seen on Figure 9e for ZnCu/Cu-Na60 and Figure 9f for ZnCu/Cu-Na200, due probably to the   low concentration of $CuCl_2$ (0.0015 M) in deposited bath. Figure 9g corresponds to Zn/Cu-H60 and Figure 9h corresponds to Zn/Cu-H200, Zn/Cu-H60 and Zn/Cu-H200 have bulky structures with average particle sizes of 1-4 μm and 4-10 μm, respectively. It is suggested that bulky structure is formed because of high Zn ion near the electrocatalyst surface while electrodeposition [6] may be the result of high $ZnCl_2$ concentration (0.2 M) was used in deposited bath. Increasing deposition time resulted in increased particle size of Zn/Cu-H. However, when Cu ion was simultaneously added in the HCl bath with Zn ion, another form of dendritic structure was observed as shown in Figure 9i for ZnCu/Cu-H60 and Figure 9j for ZnCu/Cu-H200. In this case, deposition time does not affect the dendritic morphology of ZnCu/Cu-H. But Cu ion in deposited bath can change morphology from bulky structure to be dendritic structure. When Cu was added, conditions of low concentration regions of Zn ion near electrocatalyst surface may occurred because Cu ions can compete with Zn ions for deposition on Cu foil and Cu that is deposited on Cu foil also accelerates the formation of hydrogen gas during electrodeposition method. In addition, Cu has higher hydrogen bond strength than Zn [8] so, hydrogen gas that occurs during electrodeposition also compete with Zn ion, resulting in Zn ion being more difficult to move to the electrocatalyst surface. The conditions of low concentration regions of Zn ion near electrocatalyst surface promotes the formation of dendritic structure, to grow outward toward high concentration regions of Zn ion. It can be noticed that the particle size of the dendritic structure in the case of ZnCu/Cu-HCl bath is bigger than those formed under NaCl bath because of the higher concentration of $ZnCl_2$ in deposited bath.

Figure 9 SEM images of (a) Zn foil, (b) Cu foil, (c) Zn/Cu-Na60, (d) Zn/Cu-Na200, (e)
ZnCu/Cu-Na60, (f) ZnCu/Cu-Na200, (g) Zn/Cu-H60, (h) Zn/Cu-H200, (i) ZnCu/Cu-H60
and (j) ZnCu/Cu-H200

S3400 15.0kV 8.2mm x2.00k SE   20.0um

S3400 15.0kV 8.1mm x2.00k SE   20.0um

Figure 7 SEM images of (a) Zn foil, (b) Cu foil, (c) Zn/Cu-Na60, (d) Zn/Cu-Na200, (e) ZnCu/Cu-Na60, (f) ZnCu/Cu-Na200, (g) Zn/Cu-H60, (h) Zn/Cu-H200, (i) ZnCu/Cu-H60 and (j) ZnCu/Cu-H200

S3400 15.0kV 8.5mm x2.00k SE 20.0um

S3400 15.0kV 8.6mm x2.00k SE 20.0um

Figure 7 SEM images of (a) Zn foil, (b) Cu foil, (c) Zn/Cu-Na60, (d) Zn/Cu-Na200, (e) ZnCu/Cu-Na60, (f) ZnCu/Cu-Na200, (g) Zn/Cu-H60, (h) Zn/Cu-H200, (i) ZnCu/Cu-H60 and (j) ZnCu/Cu-H200

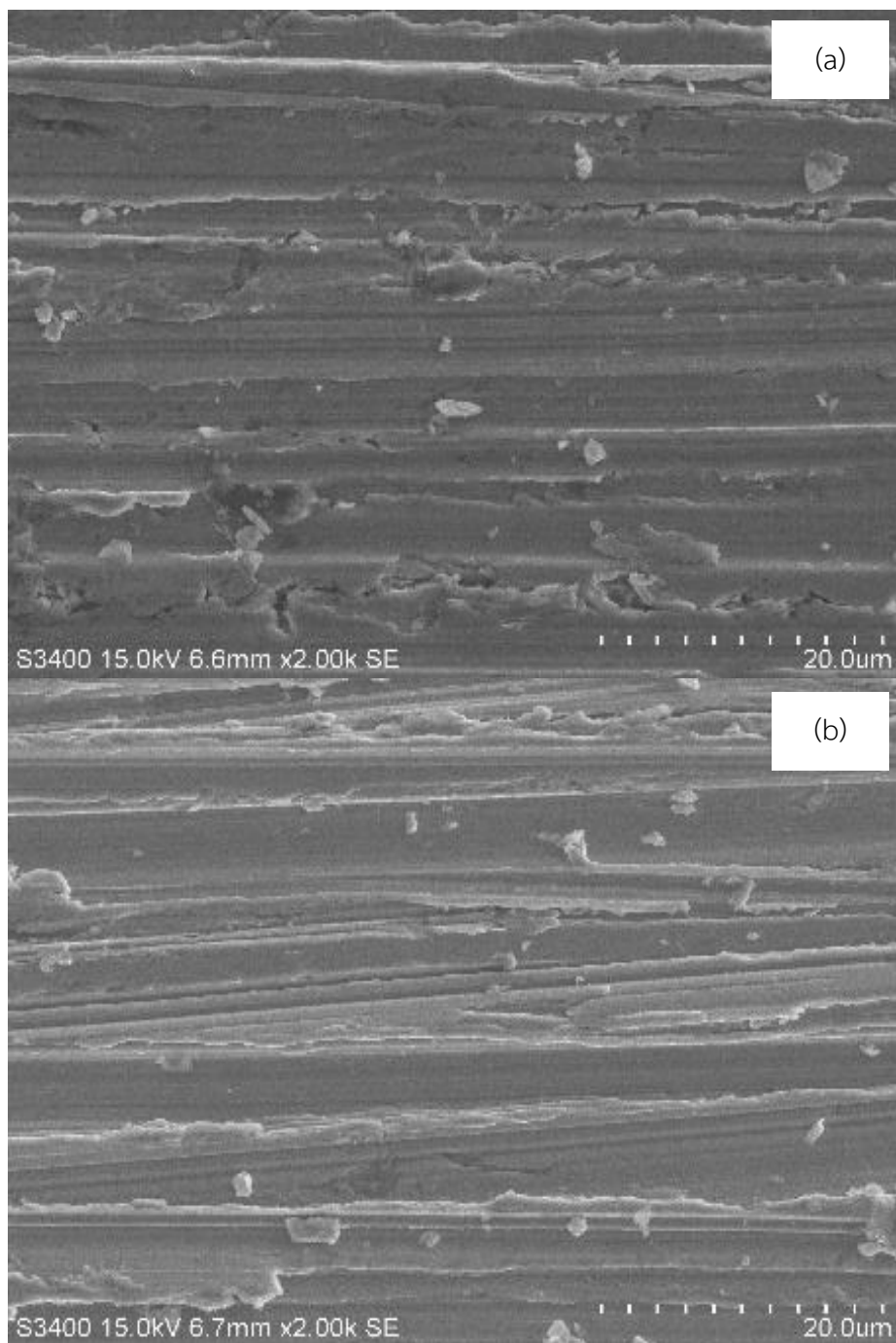Figure 7 SEM images of (a) Zn foil, (b) Cu foil, (c) Zn/Cu-Na60, (d) Zn/Cu-Na200, (e) ZnCu/Cu-Na60, (f) ZnCu/Cu-Na200, (g) Zn/Cu-H60, (h) Zn/Cu-H200, (i) ZnCu/Cu-H60 and (j) ZnCu/Cu-H200
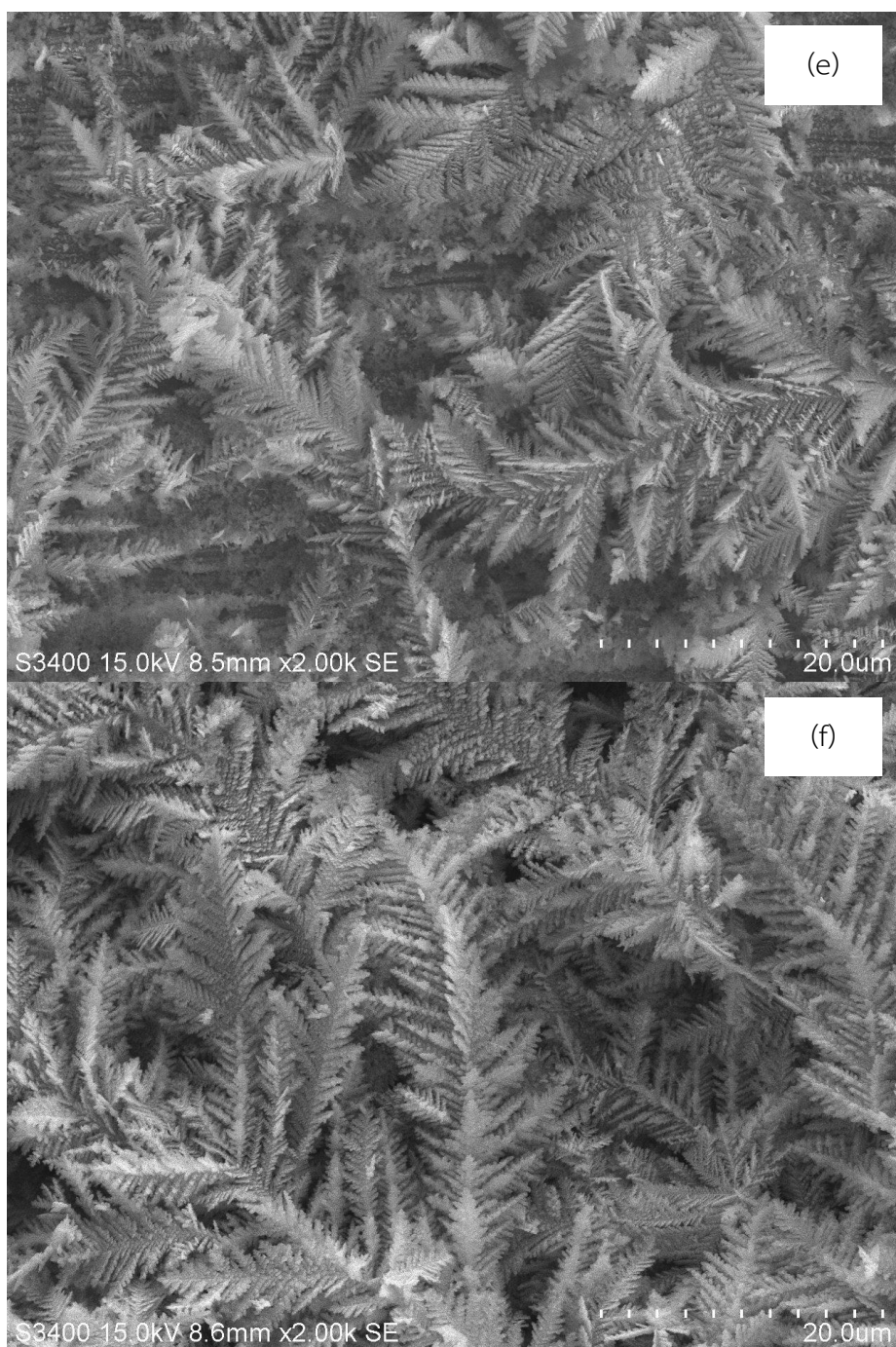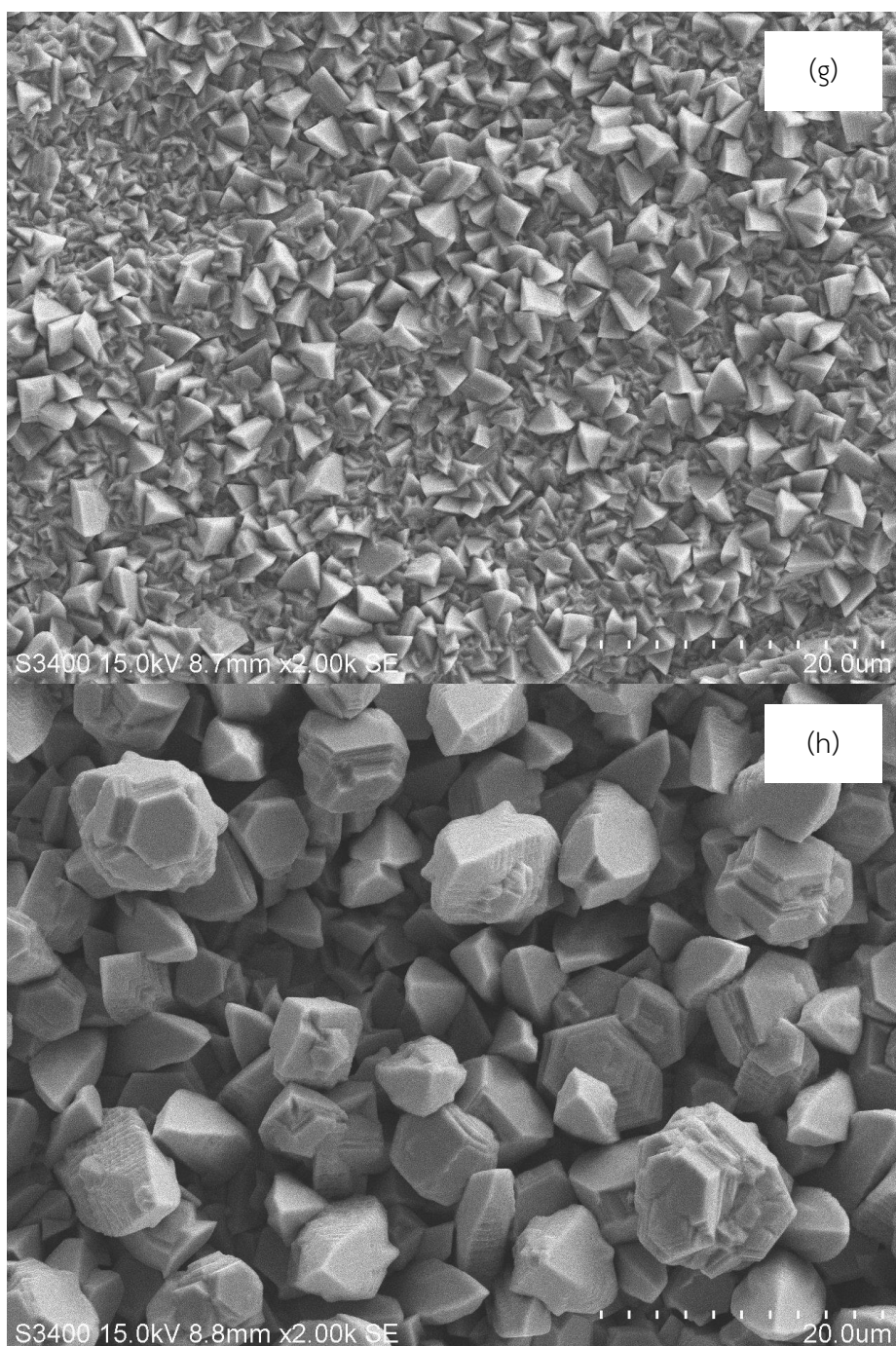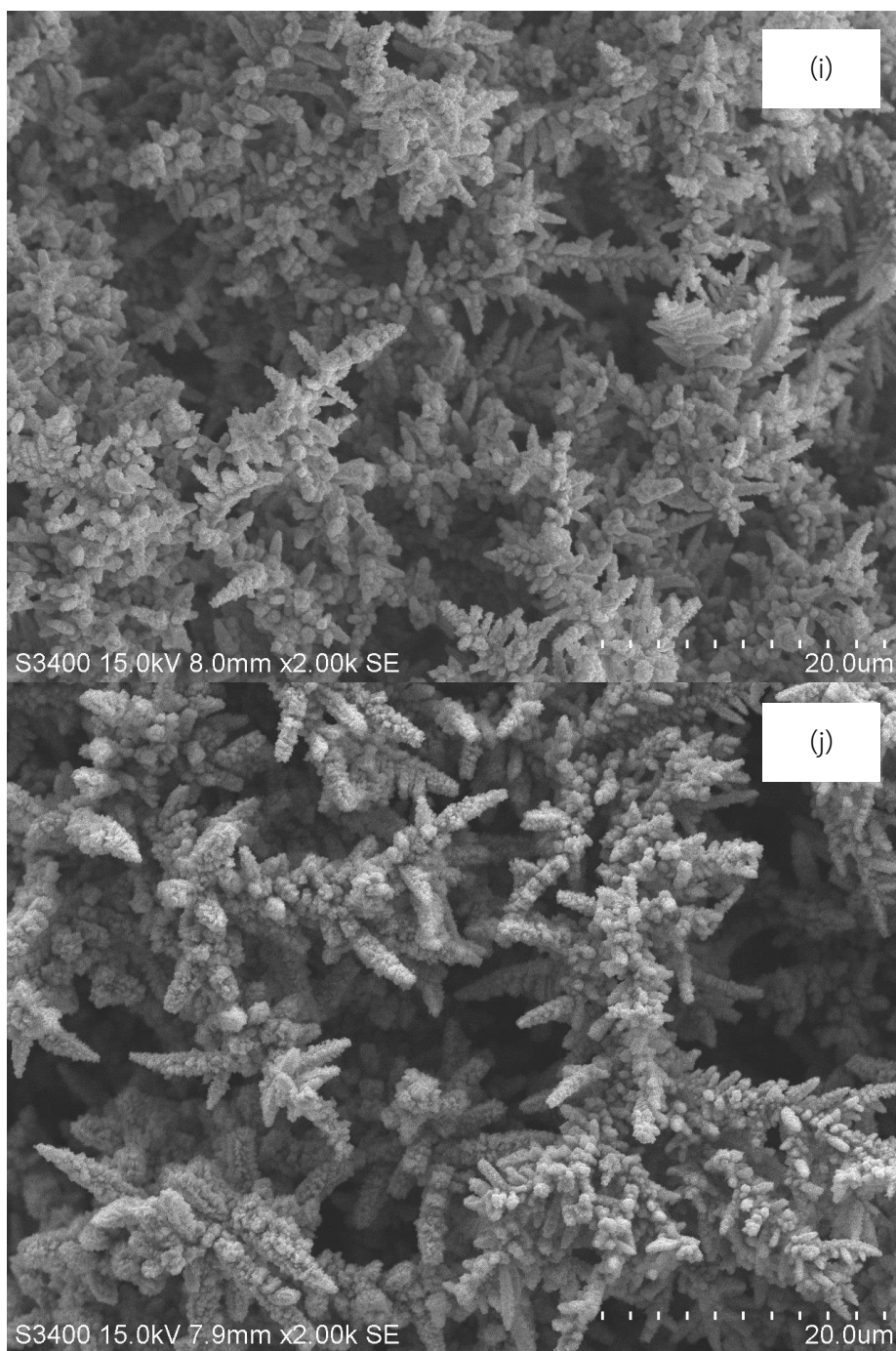
Figure 7 SEM images of (a) Zn foil, (b) Cu foil, (c) Zn/Cu-Na60, (d) Zn/Cu-Na200, (e) ZnCu/Cu-Na60, (f) ZnCu/Cu-Na200, (g) Zn/Cu-H60, (h) Zn/Cu-H200, (i) ZnCu/Cu-H60 and (j) ZnCu/Cu-H200

4.2 Activity test in the electrochemical CO_2 reduction

Table 12 The catalytic performances of Zn foil, Cu foil and Zn/Cu alloy electrocatalysts with different deposition times

Entry	Electrocatalyst	Rate (μmol/min)				CO/H_2
		CO	H_2	formate	n-Propanol	rate ratio
1	Zn foil	0.87	0.21	0.07	0.04	4.1
2	Cu foil	0.96	2.21	0.48	0.15	0.4
3	Zn/Cu-Na60	2.93	0.92	0.13	0.06	3.2
4	Zn/Cu-Na200	3.61	0.77	0.09	0.06	4.7
5	ZnCu/Cu-Na60	3.28	0.93	0.05	0.04	3.5
6	ZnCu/Cu-Na200	4.72	1.29	0.06	0.03	3.7
7	Zn/Cu-H60	0.65	0.45	0.36	-	1.5
8	Zn/Cu-H200	1.01	0.54	0.36	-	1.8
9	ZnCu/Cu-H60	3.21	0.89	0.13	0.02	3.6
10	ZnCu/Cu-H200	4.14	1.63	0.16	0.02	2.5

Reaction (Electrolyte: 0.1 M $KHCO_3$) at potential -1.6 V vs. Ag/AgCl in 70 minutes

Under potential at -1.6 V vs. Ag/AgCl, the working electrodes including Zn foil, Cu foil, Zn/Cu-Na60, Zn/Cu-Na200, ZnCu/Cu-Na60, ZnCu/Cu-Na200, Zn/Cu-H60, Zn/Cu-H200, ZnCu/Cu-H60, and ZnCu/Cu-H200 were tested in the electrochemical reduction of CO_2 for 70 minutes. The molar flow rate of the products including CO, H_2, formate and n-propanol are shown in Table 12. The CO molar flow rate using Cu foil is slightly higher than Zn foil because resistance of Cu metal is lower than resistance of Zn metal. Thus, potential that is lost with resistance of Cu metal is lower than Zn metal, resulting in the faster rate of transfer of proton/electron pair to the surface of the working electrode. The higher amount of reactants on Cu foil resulted in the formation of higher hydrocarbon products (CO, formate, and n-propanol) whereas Cu foil still produced more H_2 gas. Thus, CO/H_2 rate ratio of Cu foil is low. Formate molar flow rate of Cu foil is higher than Zn foil. That can be

rationalized by two effects: First, resistance of Cu metal is lower than Zn metal as described above. Second, Theoretical limiting potentials of Cu metal for formate production is lower than Zn metal [54]. As a consequence, Cu foil can easily produce formate than Zn foil. In case of Zn foil, the major product is CO. Owing to the fact that Zn binds CO more weakly so that CO was rapidly released from Zn surface before occurring CO reduction reaction [13]. n-Propanol molar flow rate of Cu foil is higher than Zn foil about 4 times. Because Cu possesses higher binding energy for CO than Zn, the CO product can be further reduced to other products such as n-propanol [13]. Deposited electrocatalysts exhibited higher total molar flow rate than Zn foil because deposited electrocatalysts have higher surface area than Zn foil. In case of Zn/Cu-Na60, Zn particles may not sufficiently cover on Cu substrate. As observed from percent by weight of Cu of Zn/Cu-Na60 (25.1%) that is still high when compared with Zn/Cu-Na200 (7.1%), of the presence of Cu substrate on Zn/Cu-Na60 may be the reason for higher H_2 being produced than Zn/Cu-Na200. Because the theoretical limiting potentials of Cu metal for H_2 production is lower than Zn metal [54], Zn/Cu-Na60 can easily produce H_2 than Zn/Cu-Na200. Comparing the electrodepositing Zn/Cu catalysts prepared in NaCl bath with different deposition times, CO molar flow rate is higher for the one prepared with longer deposition time (Zn/Cu-Na200) as compared to Zn/Cu-Na60. The reaction results are correlated well with the higher surface area of Zn/Cu-Na200 than Zn/Cu-Na60. Both Zn/Cu-Na60 and Zn/Cu-Na200 have similar dendritic structure, so surface area of Zn particles that are deposited on Cu foil increased with increasing deposition time. For the bimetallic ZnCu on Cu foil prepared in NaCl bath with 60 s deposition time, CO and H_2 molar flow rate of ZnCu/Cu-Na60 is not much different from Zn/Cu-Na60, due probably to the low concentration of $CuCl_2$ (0.0015 M) in deposited bath and low deposited current (20 mA/cm^2) so the catalysts exhibited similar characteristics and activity in CO_2 electrochemical reduction. However, for those prepared with 200 s deposition time (ZnCu/Cu-Na200), CO and H_2 molar flow rate of ZnCu/Cu-Na200 is found to be higher than Zn/Cu-Na200 but CO/H_2 rate ratio is lower than Zn/Cu-Na200 owing to Cu particles deposited on Cu foil leading to the increase of H_2. The higher CO molar flow rate in case of Zn/Cu-H200 compared to Zn/Cu-H60 is maybe due to the higher

surface area of Zn/Cu-H200 than Zn/Cu-H60 as the deposition time increases. However, among the other deposited electrocatalysts, the total molar flow rate of Zn/Cu-H60 and Zn/Cu-H200 is relatively low, suggesting the influence of low surface area bulky structure of the Zn/Cu-H60 and Zn/Cu-H200 on the electrochemical reduction activity [6]. Nevertheless, the production of formate on Zn/Cu-H60 and Zn/Cu-H200 is outstanding although the molar flow rate of CO and H_2 is lower than the other deposited electrocatalysts. It is possible that the bulky structure may possess more hexagonal close pack (0001) facet that promotes formate production via reduction of HCOO* intermediate. This pathway leads to the production of formate with limited formation of CO and H_2 [54]. For the ZnCu/Cu-H60 and ZnCu/Cu-H200, the molar flow rate of CO and H_2 increases as deposition time increases with ZnCu/Cu-H200 producing large amount of H_2. Among the electrocatalysts studied, Zn/Cu-Na200 is the best electrocatalyst to provide the highest CO/H_2 rate ratio about 4.7 because dendritic structure of Zn/Cu-Na200 has a higher density of stepped sites that suppress hydrogen evolution [6]. Zn/Cu-Na200 was selected to be further tested in part II. In 2015 [6], it was reported that Zn dendrite electrode showed CO/H_2 ratio about 4 that is lower than Zn/Cu-Na200 in this work may be the result of higher concentration of electrolyte (0.5 M $NaHCO_3$). Higher cat ion (Na^+) will block the adsorption of CO_2 on working electrode [55].

Part II. To identify appropriate potential and stability of the best one Zn/Cu alloy electrocatalyst that gets the highest CO/H_2 rate ratio from part I.

4.3 Activity test of Zn/Cu-Na200 in the electrochemical CO_2 reduction at various potential

Table 13 The catalytic performances of Zn/Cu-Na200 at various potentials

Entry	Potential (V vs. Ag/AgCl)	Rate (μmol/min)				CO/H_2 rate ratio
		CO	H_2	formate	n-Propanol	
1	-1.4	1.08	0.48	-	0.02	2.3
2	-1.6	3.61	0.77	0.09	0.06	4.7
3	-1.8	6.98	2.95	0.10	0.06	2.4
4	-2.0	7.97	10.18	0.19	0.06	0.8

Reaction (Electrolyte: 0.1 M $KHCO_3$) in 70 minutes

Zn/Cu-Na200 is further tested at potential -1.4, -1.8 and -2.0 V vs. Ag/AgCl. The results are shown in Table 13. At potential -1.4 V vs. Ag/AgCl, CO_2 reduction products (CO and n-propanol) is relatively low and formate is not found. Owing to the relatively low potential, the transfer of proton/electron pair also is slow. Increasing negative potential to -1.6, -1.8, and -2.0 V vs. Ag/AgCl, formate is found as a liquid product and the molar flow rate of CO H_2 and formate increase with increasing negative potential. However, as the potential increases, the CO/H_2 rate ratio decreases. It is suggested that at higher negative potential, the transfer of proton/electron pair will be faster while the mass transfer of CO_2 is still unchanged, resulting in mass transport limitations at higher overpotentials [12] which causes H_2 formation. At potential -1.6, -1.8, -2.0 V vs. Ag/AgCl, the molar flow rate of n-propanol are similar. This is probable because n-propanol formation requires 18 electron reduction [50], which is very high when compared with CO and formate. CO and formate require only 2 electron reduction [50]. The CO/H_2 rate ratio is found to be

highest at potential -1.6 V vs. Ag/AgCl. So, potential -1.6 V vs. Ag/AgCl is chosen as the condition for stability test.

4.4 Scanning electron microscope-energy dispersive X-ray spectroscopy (SEM-EDX) of Zn/Cu-Na200 before and after stability test

Table 14 Percent by weight of Zn/Cu-Na200 before and after stability test

Entry	Zn/Cu-Na200	Percent by weight	
		Zn (%)	Cu (%)
1	before reaction	92.9	7.1
2	after reaction (4 h)	93.3	6.7

Zn/Cu-Na200 is further tested at potential -1.6 V vs. Ag/AgCl for 4 h. Table 14 shows the percent by weight of Zn/Cu-Na200 before and after stability test. The Zn/Cu-Na200 before and after stability test have similar percent by weight of Zn and Cu.

The scanning electron microscopic images of Zn/Cu-Na200 before and after stability test are shown in Figure 10. Figure 10a corresponds to Zn/Cu-Na200 before stability test. It has dendritic structures with a particle size of 0.2-0.5 μm. Figure 10b corresponds to Zn/Cu-Na200 after stability test. It has dendritic structures with a particle size of 0.5-1.2 μm. Particle size of Zn/Cu-Na200 after stability test is bigger than Zn/Cu-Na200 before stability test. The increase of Zn particle size may be the result of dissolution of Zn particles that are deposited on Cu foil and redeposition under CO_2 electrolysis conditions. Redeposition of Zn ion may result in larger particles. In 2015, Rosen, J. et al. also reported the redeposition of electrocatalyst under CO_2 electrolysis conditions [6].
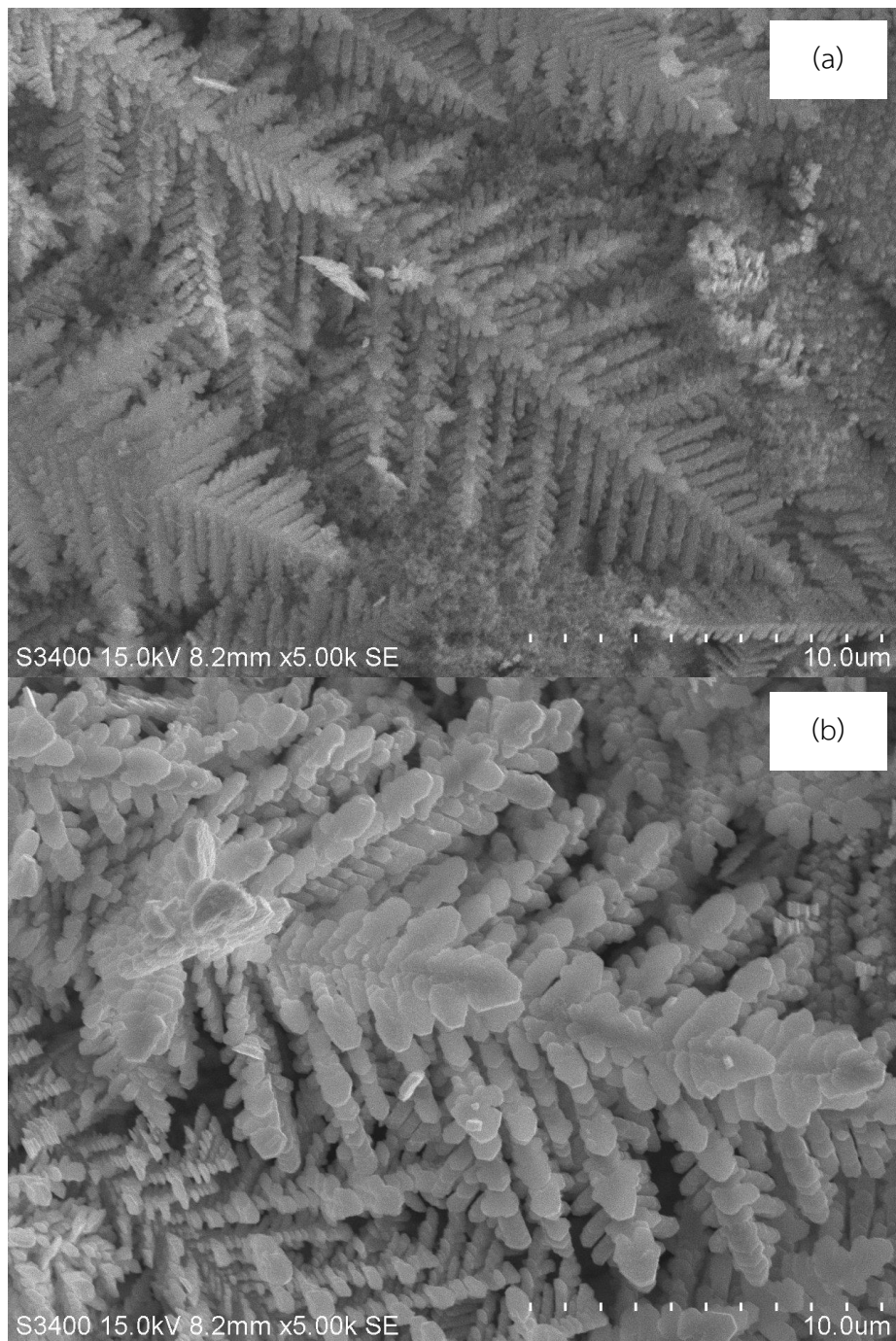
Figure 10 SEM images of Zn/Cu-Na200: (a) before and (b) after stability test

4.5 Stability test of Zn/Cu-Na200 in the electrochemical CO_2 reduction at potential -1.6 V vs Ag/AgCl

Table 15 The catalytic performances of Zn/Cu-Na200 in 4 hour

Entry	Reaction time (h)	Rate (μmol/min)	
		CO	H_2
1	1	3.55	1.25
2	2	3.66	1.32
3	3	3.53	1.32
4	4	3.47	1.58

Reaction (Electrolyte: 0.1 M $KHCO_3$) at potential -1.6 V vs. Ag/AgCl in 4 hour

Zn/Cu-Na200 is further tested at potential -1.6 V vs. Ag/AgCl for 4 h. The result is shown in Table 15. The molar flow rate of CO is relatively stable with an average value of about 3.55 μmol/min. In case of H_2, the molar flow rate of H_2 slightly increases at reaction time 4 h due probably to the result of dissolution of Zn particles that are deposited on Cu foil [6], causing more exposure of Cu substrate on the surface. The Cu substrate can produce higher H_2 because theoretical limiting potentials of Cu metal for H_2 production is lower than Zn metal [54].

CHAPTER V

CONCLUSIONS

5.1 Conclusions

Electrochemical reduction of CO_2 (ERC) using Zn/Cu-foil and ZnCu/Cu-foil electrocatalysts was investigated at ambient conditions in an H-cell type reactor. Electrodeposition of Zn on Cu foil at low Zn concentration (0.05 M) resulted in Zn dendritic structure. In case of Zn bulky structure, It was formed that may be due to high Zn concentration (0.2 M). However, when Cu ions were added simultaneously with Zn at high Zn concentration (0.2 M), dendritic structure of CuZn particles deposited on Cu-foil was observed. Adding Cu ions led to an increase of CO and H_2 products from the ERC.

Deposition time does not affect the morphology of dendritic structure. However, for the catalysts prepared using low deposition time (60 s), Zn particles may not be sufficiently covered on Cu substrate, and the exposure of Cu substrate resulted in an increase of H_2 production. Among the catalysts studied, Zn/Cu-Na200 is the best electrocatalyst that produces high CO gaseous product with low H_2 because dendritic structure of Zn/Cu-Na200 has a higher density of stepped sites that suppress hydrogen evolution. In contrast, increasing deposition time resulted in larger size of the bulky structure. The Zn bulky structure, however, produces outstanding liquid formate products. It is possible that the bulky structure may possess more hexagonal close pack (0001) facet that promotes formate production via reduction of HCOO* intermediate.

The optimized over potential was determined to be at -1.6 V vs. Ag/AgCl as the best condition for the formation of high CO while keeping low H_2 production. The activity of Zn/Cu-Na200 is quite stable during 4 h reaction test, the rate of CO production did not significantly change while H_2 production rate slightly increased. As revealed by SEM images of the catalysts after reaction, the particle size of dendritic stricture increased. It is suggested that redeposition of Zn ion occurred under CO_2 electrochemical reduction conditions.

5.2 Recommendation

      1. The increase of surface area of deposited electrocatalysts may have to be confirmed by electrochemical technique.

      2. The stability of the electrocatalysts should be investigated at longer reaction times.

REFERENCES

1. Chen, Y., C.W. Li, and M.W. Kanan, *Aqueous CO2 reduction at very low overpotential on oxide-derived Au nanoparticles.* J Am Chem Soc, 2012. **134**(49): p. 19969-72.

2. Choi, J., et al., *Electrochemical CO 2 reduction to CO on dendritic Ag–Cu electrocatalysts prepared by electrodeposition.* Chemical Engineering Journal, 2016. **299**: p. 37-44.

3. Hori, Y., *Electrochemical CO2 Reduction on Metal Electrodes*, in *Modern Aspects of Electrochemistry*, C.G. Vayenas, R.E. White, and M.E. Gamboa-Aldeco, Editors. 2008, Springer New York: New York, NY. p. 89-189.

4. Nguyen, D.L.T., et al., *Selective CO2 Reduction on Zinc Electrocatalyst: The Effect of Zinc Oxidation State Induced by Pretreatment Environment.* ACS Sustainable Chemistry & Engineering, 2017. **5**(12): p. 11377-11386.

5. Quan, F., et al., *A highly efficient zinc catalyst for selective electroreduction of carbon dioxide in aqueous NaCl solution.* Journal of Materials Chemistry A, 2015. **3**(32): p. 16409-16413.

6. Rosen, J., et al., *Electrodeposited Zn Dendrites with Enhanced CO Selectivity for Electrocatalytic CO2Reduction.* ACS Catalysis, 2015. **5**(8): p. 4586-4591.

7. Won da, H., et al., *Highly Efficient, Selective, and Stable CO2 Electroreduction on a Hexagonal Zn Catalyst.* Angew Chem Int Ed Engl, 2016. **55**(32): p. 9297-300.

8. Moreno-Garcia, P., et al., *Selective Electrochemical Reduction of CO2 to CO on Zn-Based Foams Produced by Cu(2+) and Template-Assisted Electrodeposition.* ACS Appl Mater Interfaces, 2018. **10**(37): p. 31355-31365.

9. Keerthiga, G. and R. Chetty, *Electrochemical Reduction of Carbon Dioxide on Zinc-Modified Copper Electrodes.* Journal of The Electrochemical Society, 2017. **164**(4): p. H164-H169.

10. Scibioh, M.A. and B. Viswanathan, *Electrochemical Reduction of CO 2*, in *Carbon Dioxide to Chemicals and Fuels*. 2018. p. 307-371.

11.   Gattrell, M., N. Gupta, and A. Co, *A review of the aqueous electrochemical reduction of CO2 to hydrocarbons at copper.* Journal of Electroanalytical Chemistry, 2006. **594**(1): p. 1-19.

12.   Hatsukade, T., et al., *Insights into the electrocatalytic reduction of CO(2) on metallic silver surfaces.* Phys Chem Chem Phys, 2014. **16**(27): p. 13814-9.

13.   Kuhl, K.P., et al., *Electrocatalytic conversion of carbon dioxide to methane and methanol on transition metal surfaces.* J Am Chem Soc, 2014. **136**(40): p. 14107-13.

14.   Wu, J., et al., *Electrochemical Reduction of Carbon Dioxide I. Effects of the Electrolyte on the Selectivity and Activity with Sn Electrode.* Journal of The Electrochemical Society, 2012. **159**(7): p. F353-F359.

15.   Lv, W., et al., *Studies on the faradaic efficiency for electrochemical reduction of carbon dioxide to formate on tin electrode.* Journal of Power Sources, 2014. **253**: p. 276-281.

16.   Del Castillo, A., et al., *Electrocatalytic reduction of CO2 to formate using particulate Sn electrodes: Effect of metal loading and particle size.* Applied Energy, 2015. **157**: p. 165-173.

17.   Zhang, R., W. Lv, and L. Lei, *Role of the oxide layer on Sn electrode in electrochemical reduction of CO 2 to formate.* Applied Surface Science, 2015. **356**: p. 24-29.

18.   Zhao, C. and J. Wang, *Electrochemical reduction of CO 2 to formate in aqueous solution using electro-deposited Sn catalysts.* Chemical Engineering Journal, 2016. **293**: p. 161-170.

19.   Wang, Y., et al., *Electrochemical reduction of CO2 to formate catalyzed by electroplated tin coating on copper foam.* Applied Surface Science, 2016. **362**: p. 394-398.

20.   Yu, J., et al., *Electrochemical reduction of carbon dioxide at nanostructured SnO 2 /carbon aerogels: The effect of tin oxide content on the catalytic activity and formate selectivity.* Applied Catalysis A: General, 2017. **545**: p. 159-166.

21.   Li, F., et al., *Towards a better Sn: Efficient electrocatalytic reduction of CO 2 to formate by Sn/SnS 2 derived from SnS 2 nanosheets.* Nano Energy, 2017. **31**: p.

270-277.

22. Jiang, H., et al., *Electrochemical CO2 reduction to formate on Tin cathode: Influence of anode materials.* Journal of CO2 Utilization, 2018. **26**: p. 408-414.

23. Ge, H., et al., *Mesoporous tin oxide for electrocatalytic CO2 reduction.* J Colloid Interface Sci, 2018. **531**: p. 564-569.

24. Wang, X., et al., *Nanoporous Ag-Sn derived from codeposited AgCl-SnO2 for the electrocatalytic reduction of CO2 with high formate selectivity.* Electrochemistry Communications, 2019. **102**: p. 52-56.

25. Rasul, S., et al., *Low cost and efficient alloy electrocatalysts for CO2 reduction to formate.* Journal of CO2 Utilization, 2019. **32**: p. 1-10.

26. Kim, Y.E., et al., *Leaching-resistant SnO2/ɣ-Al2O3 nanocatalyst for stable electrochemical CO2 reduction into formate.* Journal of Industrial and Engineering Chemistry, 2019. **78**: p. 73-78.

27. Yang, H., et al., *Selective electrocatalytic CO2 reduction enabled by SnO2 nanoclusters.* Journal of Energy Chemistry, 2019. **37**: p. 93-96.

28. Sarfraz, S., et al., *Cu–Sn Bimetallic Catalyst for Selective Aqueous Electroreduction of CO2 to CO.* ACS Catalysis, 2016. **6**(5): p. 2842-2851.

29. Zeng, J., et al., *Advanced Cu-Sn foam for selectively converting CO2 to CO in aqueous solution.* Applied Catalysis B: Environmental, 2018. **236**: p. 475-482.

30. Li, Q.-y., et al., *Electrochemical reduction of CO 2 into CO in N -methyl pyrrolidone/tetrabutylammonium perchlorate in two-compartment electrolysis cell.* Journal of Electroanalytical Chemistry, 2017. **785**: p. 229-234.

31. Shi, J., et al., *Electrochemical reduction of CO2 into CO in tetrabutylammonium perchlorate/propylene carbonate: Water effects and mechanism.* Electrochimica Acta, 2017. **240**: p. 114-121.

32. Kim, J.-H., et al., *Highly active and selective Au thin layer on Cu polycrystalline surface prepared by galvanic displacement for the electrochemical reduction of CO2 to CO.* Applied Catalysis B: Environmental, 2017. **213**: p. 211-215.

33. Chen, C., et al., *Selective electrochemical CO2 reduction over highly porous gold films.* J. Mater. Chem. A, 2017. **5**(41): p. 21955-21964.

34. Cave, E.R., et al., *Electrochemical CO2 reduction on Au surfaces: mechanistic aspects regarding the formation of major and minor products.* Phys Chem Chem Phys, 2017. **19**(24): p. 15856-15863.

35. Shen, F.-x., et al., *Electrochemical reduction of CO2 to CO over Zn in propylene carbonate/tetrabutylammonium perchlorate.* Journal of Power Sources, 2018. **378**: p. 555-561.

36. Park, G., et al., *Au on highly hydrophobic carbon substrate for improved selective CO production from CO2 in gas-phase electrolytic cell.* Catalysis Today, 2019.

37. Ahangari, H.T., T. Portail, and A.T. Marshall, *Comparing the electrocatalytic reduction of CO2 to CO on gold cathodes in batch and continuous flow electrochemical cells.* Electrochemistry Communications, 2019. **101**: p. 78-81.

38. Lee, H., S.-K. Kim, and S.H. Ahn, *Electrochemical preparation of Ag/Cu and Au/Cu foams for electrochemical conversion of CO2 to CO.* Journal of Industrial and Engineering Chemistry, 2017. **54**: p. 218-225.

39. Ma, L., et al., *Polyvinyl alcohol-modified gold nanoparticles with record-high activity for electrochemical reduction of CO2 to CO.* Journal of CO2 Utilization, 2019. **34**: p. 108-114.

40. Kim, B., et al., *Influence of dilute feed and pH on electrochemical reduction of CO2 to CO on Ag in a continuous flow electrolyzer.* Electrochimica Acta, 2015. **166**: p. 271-276.

41. Park, H., et al., *AgIn dendrite catalysts for electrochemical reduction of CO2 to CO.* Applied Catalysis B: Environmental, 2017. **219**: p. 123-131.

42. Ham, Y.S., et al., *Electrodeposited Ag catalysts for the electrochemical reduction of CO 2 to CO.* Applied Catalysis B: Environmental, 2017. **208**: p. 35-43.

43. Ham, Y.S., et al., *Direct formation of dendritic Ag catalyst on a gas diffusion layer for electrochemical CO2 reduction to CO and H2.* International Journal of Hydrogen Energy, 2018. **43**(24): p. 11315-11325.

44. Lee, H., et al., *Nanostructured Ag/In/Cu foam catalyst for electrochemical reduction of CO2 to CO.* Electrochimica Acta, 2019. **323**.

45. Rudnev, A.V., et al., *Enhanced electrocatalytic CO formation from CO2 on nanostructured silver foam electrodes in ionic liquid/water mixtures.* Electrochimica Acta, 2019. **306**: p. 245-253.

46. Lu, Y., et al., *Efficient electrocatalytic reduction of CO2 to CO on an electrodeposited Zn porous network.* Electrochemistry Communications, 2018. **97**: p. 87-90.

47. Zhang, T., et al., *Multilayered Zn nanosheets as an electrocatalyst for efficient electrochemical reduction of CO2.* Journal of Catalysis, 2018. **357**: p. 154-162.

48. Morimoto, M., et al., *Visualization of catalytic edge reactivity in electrochemical CO2 reduction on porous Zn electrode.* Electrochimica Acta, 2018. **290**: p. 255-261.

49. Zhen, J.-Z., et al., *Fabrication of ZnS/Zn electrode using sulphur infiltration method for CO2 reduction into CO in organic media.* Journal of Alloys and Compounds, 2019. **771**: p. 994-999.

50. Kuhl, K.P., et al., *New insights into the electrochemical reduction of carbon dioxide on metallic copper surfaces.* Energy & Environmental Science, 2012. **5**(5).

51. Xie, J., Y. Huang, and H. Yu, *Tuning the catalytic selectivity in electrochemical CO2 reduction on copper oxide-derived nanomaterials.* Frontiers of Environmental Science & Engineering, 2014. **9**(5): p. 861-866.

52. Sobha Jayakrishnan, D., *Electrodeposition: the versatile technique for nanomaterials*, in *Corrosion Protection and Control Using Nanomaterials*. 2012. p. 86-125.

53. Katoh, A., *Design of Electrocatalyst for CO[sub 2] Reduction.* Journal of The Electrochemical Society, 1994. **141**(8): p. 2054.

54. Yoo, J.S., et al., *Theoretical Insight into the Trends that Guide the Electrochemical Reduction of Carbon Dioxide to Formic Acid.* ChemSusChem, 2016. **9**(4): p. 358-63.

55. Zhong, H., K. Fujii, and Y. Nakano, *Effect of KHCO3Concentration on Electrochemical Reduction of CO2on Copper Electrode.* Journal of The

Electrochemical Society, 2017. **164**(9): p. F923-F927.

APPENDIX

APPENDIX A

SCANNING ELECTRON MICROSCOPY

Zn/Cu-H is further deposited by deposition time 500 s and 1000 s. Scanning electron microscopic images of Zn/Cu-H500 and Zn/Cu-H1000 are shown in Figure A.1.
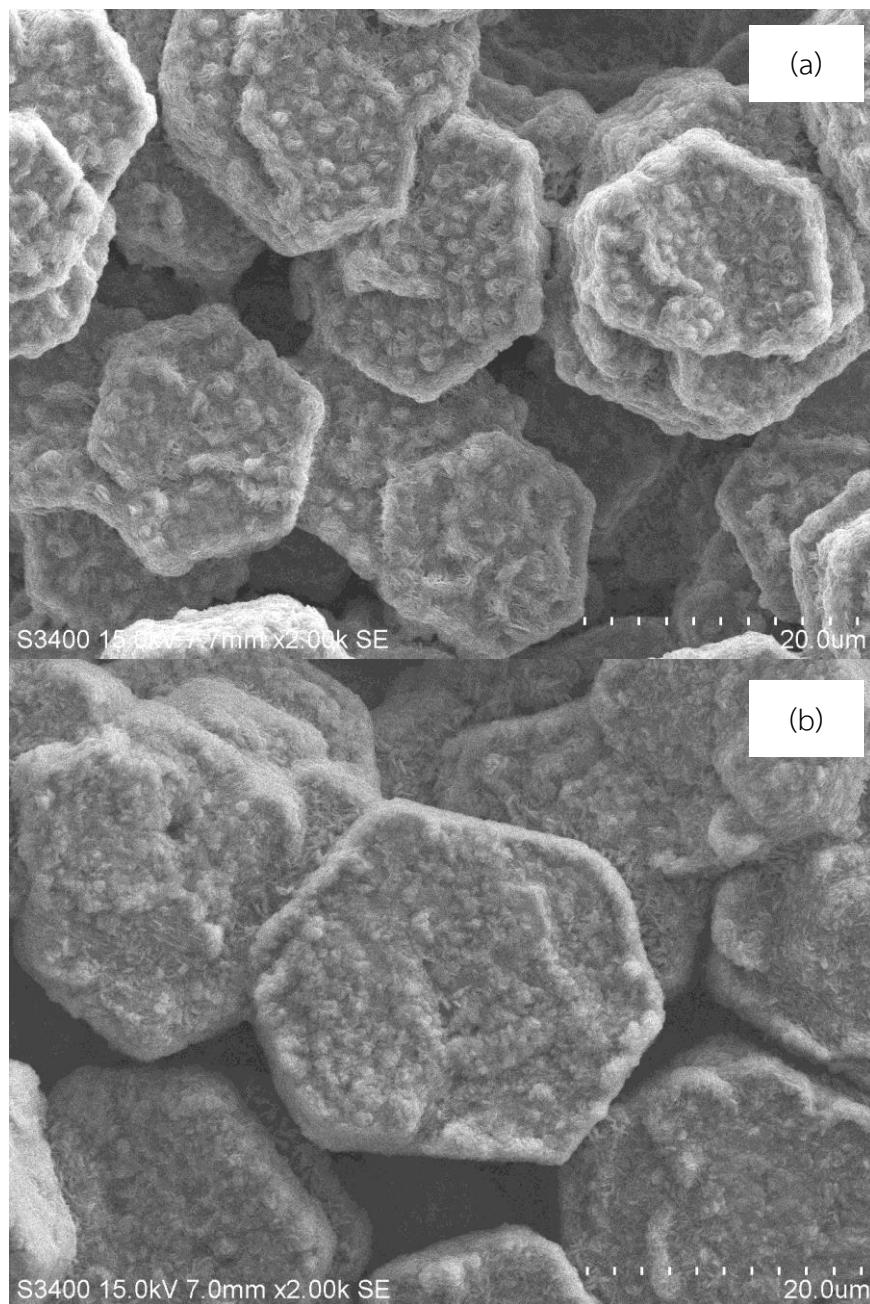

Figure A.1 SEM images of (a) Zn/Cu-H500 and (b) Zn/Cu-H1000
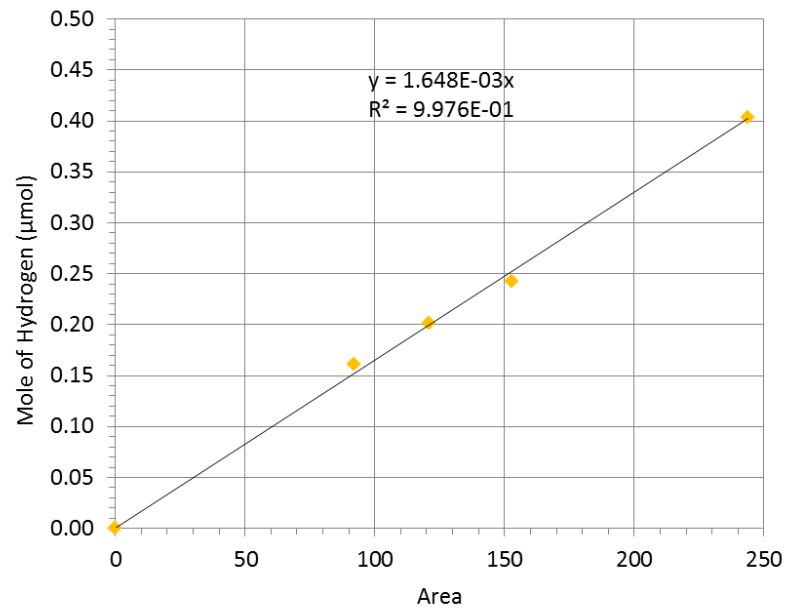
APPENDIX B

THE CALIBRATION CURVE OF GAS PRODUCT
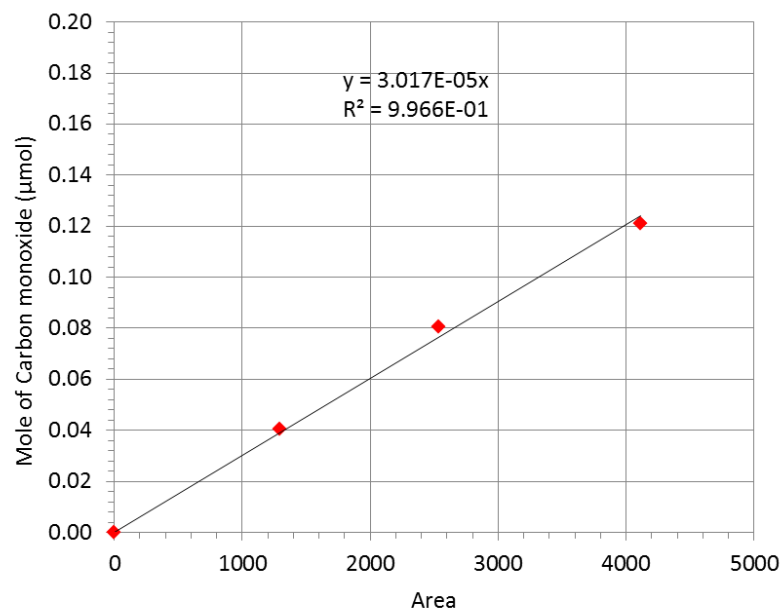

Figure B.1 The calibration curve of hydrogen

Figure B.2 The calibration curve of hydrogen

APPENDIX C

THE LIQUID PRODUCT IDENTIFICATION FOR NMR ANALYSIS

Table C.1 The liquid product identification for NMR analysis [50].

Product name	^{1}H splitting	Chemical Shift
Formate	s	8.33
DMSO (Internal Standard)	s	2.6
n-Propanol	t	0.77

จุฬาลงกรณ์มหาวิทยาลัย

CHULALONGKORN UNIVERSITY

VITA

NAME	Phongsathon Klongklaew
DATE OF BIRTH	18 September 1995
PLACE OF BIRTH	Songkhla, Thailand
INSTITUTIONS ATTENDED	B.Eng Chemical Engineering Faculty of Engineering, Prince of Songkla University
HOME ADDRESS	25/18 Tesapattana Road, Hatyai Subdistrict, Hatyai District, Songkhla Province, 90110

จุฬาลงกรณ์มหาวิทยาลัย
CHULALONGKORN UNIVERSITY